

## Hydroformylation in Room Temperature Ionic Liquids (RTILs): Catalyst and Process Developments

Marco Haumann, and Anders Riisager

*Chem. Rev.*, **2008**, 108 (4), 1474-1497 • DOI: 10.1021/cr078374z

Downloaded from <http://pubs.acs.org> on December 24, 2008

### More About This Article

---

Additional resources and features associated with this article are available within the HTML version:

- Supporting Information
- Links to the 3 articles that cite this article, as of the time of this article download
- Access to high resolution figures
- Links to articles and content related to this article
- Copyright permission to reproduce figures and/or text from this article

[View the Full Text HTML](#)



**ACS Publications**  
High quality. High impact.

# Hydroformylation in Room Temperature Ionic Liquids (RTILs): Catalyst and Process Developments

Marco Haumann\*<sup>†</sup> and Anders Riisager\*<sup>‡</sup>

Lehrstuhl für Chemische Reaktionstechnik, Universität Erlangen-Nürnberg, Egerlandstrasse 3, D-91058 Erlangen, Germany, and Department of Chemistry and Center for Sustainable and Green Chemistry, Technical University of Denmark, Building 207, DK-2800 Kgs. Lyngby, Denmark

Received July 18, 2007

## Contents

1. Introduction	1474
2. Solubility of Hydroformylation Relevant Compounds in Ionic Liquids	1476
2.1. Hydrogen and Carbon Monoxide Solubility	1476
2.2. Ethene, Propene, and 1-Butene Solubility	1477
2.3. Alcohol and Aldehyde Solubility	1477
3. Biphasic Hydroformylation with Ionic Liquids	1478
3.1. Ionic Liquid Progression	1478
3.2. Progression in Ligand Design	1483
3.2.1. Achiral Ligands	1483
3.2.2. Chiral Ligands	1485
3.3. Carbon Dioxide as an Alternative Source of CO	1486
4. Spectroscopic and Mechanistic Studies of Hydroformylation Catalysts in Ionic Liquids	1487
4.1. Rhodium Complex Catalysts	1487
4.2. Platinum Complex Catalysts	1489
5. Hydroformylation with Ionic Liquids in Alternative Reaction Systems	1490
5.1. Supported Ionic Liquid-Phase (SILP) Systems	1490
5.1.1. Batch Mode Reactions	1490
5.1.2. Continuous Flow Reactions	1491
5.2. Ionic Liquid–Supercritical CO <sub>2</sub> Systems	1493
5.2.1. Biphasic-Catalyzed Reactions	1493
5.2.2. SILP-Catalyzed Reactions	1495
6. Concluding Comments	1495
7. Acknowledgements	1496
8. References	1496

## 1. Introduction

Over the last few years, ionic liquids have successfully been applied as alternative solvents for homogeneous biphasic catalysis.<sup>1–5</sup> Many transition metal complexes dissolve readily in ionic liquids, which enables their use as solvents for transition metal catalysis. Sufficient solubility for a wide range of catalyst complexes is an obvious, but not trivial, prerequisite for a versatile solvent for homogeneous catalysis. Obviously, there are many other good reasons to apply ionic

liquids as alternative solvents in transition metal-catalyzed reactions. Besides their very low vapor pressure and their good thermal stability, an important advantage is the possibility to tune their solubility and acidity/coordination properties by varying the nature of the anions and cations systematically.<sup>6</sup> The possibility of adjusting solubility properties is of particular importance for liquid–liquid biphasic catalysis. Liquid–liquid catalysis can be realized when one liquid is able to dissolve the catalyst and displays a partial solubility with the substrates and a poor solubility with the reaction products. Under these conditions, the product phase, containing also the unconverted reactants, is removed by simple phase decantation and the liquid containing the catalyst can be recycled. In hydroformylation, this concept has been successfully applied for reactions of short alkenes in the Ruhrchemie/Rhône-Poulenc Process (RCH/RP).<sup>7–9</sup>

In an ideal biphasic reaction scenario, the ionic catalyst solution may be seen as an investment for a potential technical process or as a “working solution” if only a small amount has to be replaced after a certain time of application. In this connection, an essential aspect is related to the thermal and chemical stability of the ionic liquid solvent under the applied reaction conditions. While most dry ionic liquids have good thermal stability, often with decomposition temperatures of 200 °C or more, the presence of water in reaction systems may result in ionic liquid degradation by hydrolysis.<sup>10</sup> Particular ionic liquids with chloroaluminate and [PF<sub>6</sub>]<sup>−</sup> anions are known to easily undergo hydrolysis, with the latter forming phosphates and HF acid, which unintentionally may contribute to acid-catalyzed reactions or initiate catalyst degradation.<sup>11</sup> In this connection, it is worth noting that numerous reactions, well-known to be catalyzed by protic acids, have been reported to proceed rapidly in ionic liquids with [PF<sub>6</sub>]<sup>−</sup> anions.<sup>12</sup> Similarly, many results obtained with [PF<sub>6</sub>]<sup>−</sup>-containing reaction systems rich in water have most probably been under the influence of partial catalyst degradation. This, of course, suggests that the use of [PF<sub>6</sub>]<sup>−</sup> ionic liquids, and other known hydrolysis labile ionic liquids, should generally be avoided in reaction systems containing water. Also, results obtained with reactions involving low-valent metals, which are found to catalyze [PF<sub>6</sub>]<sup>−</sup> degradation with formation of transition metal fluorides, should only be treated with due circumspection.<sup>13</sup>

Another important aspect of the biphasic reaction concept is the immobilization of the transition metal catalyst in the ionic liquid. While most transition metal catalysts easily dissolve in an ionic liquid without a special ligand design, ionic ligand systems have been applied with great success

\* To whom correspondence should be addressed. A.R.: phone, +45 45252233; fax, +45 45883136; e-mail, ar@kemi.dtu.dk. M.H.: phone, +49 9131 8527429; fax, +49 9131 8527421; e-mail, haumann@crt.cbi.uni-erlangen.de.

<sup>†</sup> Universität Erlangen-Nürnberg.

<sup>‡</sup> Technical University of Denmark.



Marco Haumann was born in 1969 in Dortmund, Germany. After preliminary studies in mechanical engineering in Dortmund, he moved to TU Berlin, where he studied chemistry until 1998. He finished his Ph.D. thesis in the group of Prof. Schomäcker on hydroformylation in microemulsions in 2001. In 2002 he started a postdoctoral research project funded by Sasol Technology, Pty, Ltd. at the University of Cape Town (Prof. John R. Moss) aiming at the synthesis of novel cobalt-based catalysts. At the end of 2002 he moved to the University of Johannesburg (Prof. Andre Roodt) to study the mechanism of cobalt phosphite-catalyzed hydroformylation. Since December of 2003 he has been employed as a research assistant in the group of Prof. Peter Wasserscheid. His main research interests are in the field of homogeneous catalyst immobilization using the supported ionic liquid phase (SILP) concept and reaction engineering aspects of this innovative technology.



Anders Riisager was born in 1973 in Glostrup, Denmark. He obtained his M.Sc. in inorganic chemistry at the University of Copenhagen in 1999. In 2002 he finished his Ph.D. on the study of new immobilized biphasic hydroformylation catalyst systems (e.g., SILP) at the Interdisciplinary Research Center for Catalysis and the Department of Chemistry at the Technical University of Denmark (DTU). In the period 2002–2005 he continued work on SILP catalysis and other phase-separable ionic liquid systems with the group of Prof. Peter Wasserscheid at RWTH-Aachen (now Universität Erlangen-Nürnberg), Germany. This work was expanded in 2005–2006 via a Villum Kann Rasmussen postdoctoral fellowship and a post doc position at DTU (Prof. Rasmus Fehrmann). Since 2007 he has been employed as an Associate Professor at the institute and associated with the Center for Sustainable and Green Chemistry at DTU. His main research interests are on development of sustainable catalytic and absorption applications with ionic liquids for chemical production and environmental processes, with particular emphasis on the SILP concept.

to prevent catalyst leaching under conditions of intense mixing in continuous liquid–liquid biphasic operation.<sup>14</sup> Many of the important ligand developments have been made for the biphasic hydroformylation reaction, and a vast number of publications have shown improved potential of ionic

liquids with regard to product separation, catalyst recovery, improved catalyst stability, and selectivity.<sup>15,16</sup>

Early work by Parshall in 1972 described the use of tetraethylammonium trichlorostannate melts for the platinum-catalyzed hydroformylation of ethene.<sup>17</sup> The reaction conditions applied were harsh, with 90 °C and 400 bar syngas pressure. In 1987 Knifton reported the ruthenium- and cobalt-catalyzed hydroformylation of internal and terminal alkenes in tetra-*n*-butylphosphonium bromide melts.<sup>18</sup> The ionic medium was found to stabilize the catalyst species, indicated by improved catalyst lifetime at low syngas pressures and higher temperatures. The use of ionic liquids which are solid at room temperature was reported by Andersen and co-workers in 1998.<sup>19</sup> They used phosphonium tosylate melts for both ligand modified and unmodified rhodium hydroformylation. At 100 °C reaction temperature, these melts are liquid, and they solidify upon cooling to room temperature. Product separation was achieved by solid–liquid separation, and the catalyst recycling was reported to be complete without deactivation or rhodium leaching into the organic phase.

The first biphasic, liquid–liquid catalysis with room temperature ionic liquids was carried out by Chauvin and Olivier-Bourbigou in the mid-nineties.<sup>20</sup> However, only development and broader availability of non-chloroaluminate ionic liquids have further contributed to catalytic work in this research field starting from the late nineties. Today, a significant part of the ballooning number of publications on ionic liquid chemistry (nearly 2900 in 2006 and so far 2800 in 2007, according to SciFinder<sup>21</sup>) deals with transition metal catalysis in these unusual liquid materials. This intense research activity was documented recently by a number of quite conclusive review articles and book chapters.<sup>22–33</sup>

In this review we will focus on the development of room temperature ionic liquids as alternative solvents for biphasic catalysis, exemplified for the hydroformylation reaction. The development of novel ionic liquids as well as ligands to match the requirements of biphasic catalysis will be discussed. Mechanistic studies including in situ IR and NMR techniques will be presented to signify similarities and differences when using ionic liquids as solvents instead of molecular organic solvents, and the novel concept of supported ionic liquid-phase (SILP) catalysis and catalytic systems comprising scCO<sub>2</sub> are included to enlighten the potential of ionic liquids as optional reaction media for process designs applying continuous fixed-bed reactions. Additionally, the effect of hydrogen, carbon monoxide, ethene, propene, and 1-butene gas solubility in ionic liquids on catalyst performance in rhodium-catalyzed hydroformylation will be addressed together with alcohol and aldehyde solubility. The review will cover literature published up to December 2007.

In the review 1-alkyl-3-methyl imidazolium cations are denoted as [RMIM]<sup>+</sup>, 1-alkyl-2,3-dimethyl imidazolium cations are denoted as [RMMIM]<sup>+</sup>, *N*-alkylpyridinium cations are denoted as [RPy]<sup>+</sup>, 4-methyl-*N*-alkyl pyridinium cations are denoted as [RMPyr]<sup>+</sup>, and *N*-alkyl-*N*-methyl pyrrolidinium cations are denoted as [RMPyr]<sup>+</sup>, where R is a letter notation presenting the alkyl chain attached to the nitrogen center with M = methyl, E = ethyl, B = butyl, H = hexyl, O = octyl, and Bz = benzyl. The anion bis-(trifluoromethylsulfonyl)imide [(CF<sub>3</sub>SO<sub>2</sub>)<sub>2</sub>N]<sup>-</sup> is denoted as [Tf<sub>2</sub>N]<sup>-</sup>, and triflate [CF<sub>3</sub>SO<sub>3</sub>]<sup>-</sup> is denoted as [TfO]<sup>-</sup>.

## 2. Solubility of Hydroformylation Relevant Compounds in Ionic Liquids

### 2.1. Hydrogen and Carbon Monoxide Solubility

Various attempts have been made to determine the solubility of syngas in ionic liquids, since a nearly equimolar ratio of hydrogen and carbon monoxide is required in the liquid catalyst phase to obtain active and selective hydroformylation rhodium catalysts.<sup>34</sup>

In one of the first efforts linking gas solubility with reactivity and selectivity in biphasic ionic liquid catalysis, Dupont and co-workers in 2001 determined the hydrogen solubility and derived Henry's laws coefficient ( $k_H$ ) in [BMIM][PF<sub>6</sub>] at room temperature via a simple pressure drop in a closed vessel.<sup>35</sup> They reported a very high Henry coefficient of 5700 bar, indicative of poor hydrogen solubility in the ionic liquid (Table 1, entry 1). In 2002 Brennecke et al. tried to calculate the solubility of hydrogen and CO in several ionic liquids using a gravimetric microbalance, but low solubility prevented Henry coefficients from being determined for these low molecular weight gases.<sup>36</sup>

Henry coefficients for hydrogen solubility in various ionic liquids (only a selection is given in Table 1) were systematically determined by Dyson et al. in 2003 using high pressure <sup>1</sup>H NMR (entries 2–10).<sup>37</sup> Here, hydrogen solubility was generally found to be significantly lower than that for molecular solvents but very similar to that for water, and the Henry coefficient was largely independent of the alkyl chain length for 1-alkyl-3-methyl imidazolium tetrafluoroborate ionic liquids (entries 3–5). Pyridinium-based ionic liquids showed a slightly better solubility for hydrogen (entries 7 and 8), probably due to their lower viscosity (85 cP for [BMPyr][Tf<sub>2</sub>N] compared to 135 cP for [OMIM][BF<sub>4</sub>]). The highest hydrogen solubility was found with [P(C<sub>6</sub>H<sub>13</sub>)<sub>3</sub>(C<sub>14</sub>H<sub>29</sub>)] [PF<sub>3</sub>(C<sub>2</sub>F<sub>5</sub>)<sub>3</sub>] (entry 9), although this ionic liquid had the highest viscosity (498 cP) of all investigated ionic liquids. Notably, this solubility trend was not found in comparable hydrogenation experiments, where all ionic liquid systems exhibited similar activity. Recently, Maurer and co-workers reported the hydrogen solubility in [HMIM][Tf<sub>2</sub>N] expressed as the Henry constant on the molality scale (entries 11–17).<sup>38</sup> The hydrogen solubility was found to increase in the temperature range between 20 and 140 °C, resulting in decreased Henry constants.

Both hydrogen and CO solubility have further been determined by Gomes and co-workers using an isochoric saturation technique, where Henry constants in [BMIM][PF<sub>4</sub>] were calculated in the temperature range 5–70 °C (Table 1, entries 15–17, and Table 2, entries 32–34).<sup>39</sup> For both CO and hydrogen solubility, the authors reported a minor decrease in solubility with increasing temperature, whereas all previous studies indicated higher hydrogen solubility at higher temperatures. Dyson and co-workers used <sup>13</sup>C NMR experiments to determine the Henry coefficient of CO in various ionic liquids.<sup>40</sup> Table 2 gives a selection of the examined imidazolium ionic liquids.

For ionic liquids with the same imidazolium cation or pyridinium cation (not shown in Table 2), [Tf<sub>2</sub>N]-based ionic liquids had significantly higher CO solubility than [BF<sub>4</sub>]-based ionic liquids. For both series, the CO solubility also increased with increasing alkyl chain length of the alkyl substituent on the cation, as depicted in Figure 1, while only a marginal temperature dependence of CO solubility was

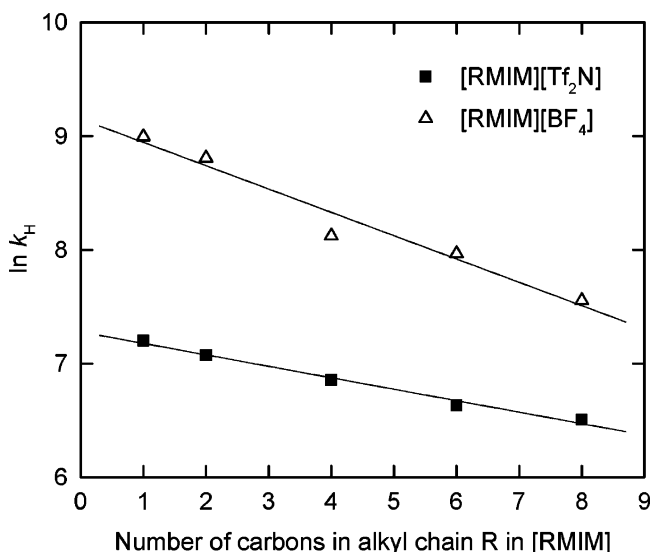
**Table 1. Hydrogen Solubility in Ionic Liquids Expressed by the Henry Coefficient (at 1 Bar)**

entry	ionic liquid	<i>T</i> (°C)	Henry coefficient, $k_H$ (bar)	ref
1	[BMIM][PF <sub>6</sub> ]	RT	5700	35
2	[BMIM][PF <sub>6</sub> ]	RT	6600	37
3	[BMIM][BF <sub>4</sub> ]	RT	5800	37
4	[HMIM][BF <sub>4</sub> ]	RT	5700	37
5	[OMIM][BF <sub>4</sub> ]	RT	6400	37
6	[BMIM][Tf <sub>2</sub> N]	RT	4500	37
7	[BPyr][Tf <sub>2</sub> N]	RT	3900	37
8	[BMPyr][Tf <sub>2</sub> N]	RT	3700	37
9	[P(C <sub>6</sub> H <sub>13</sub> ) <sub>3</sub> (C <sub>14</sub> H <sub>29</sub> )] [PF <sub>3</sub> (C <sub>2</sub> F <sub>5</sub> ) <sub>3</sub> ]	RT	700	37
10	[BMIM][TfO]	RT	4600	37
11	[HMIM][Tf <sub>2</sub> N]	RT	863	38
12	[HMIM][Tf <sub>2</sub> N]	60	701	38
13	[HMIM][Tf <sub>2</sub> N]	100	603	38
14	[HMIM][Tf <sub>2</sub> N]	140	529	38
15	[BMIM][BF <sub>4</sub> ]	RT	2036	39
16	[BMIM][BF <sub>4</sub> ]	50	2780	39
17	[BMIM][BF <sub>4</sub> ]	70	4318	39

**Table 2. Carbon Monoxide Solubility in Ionic Liquids Expressed by the Henry Coefficient (at 1 Bar)**

entry	ionic liquid	<i>T</i> (°C)	Henry coefficient, $k_H$ (bar)	ref
18	[MMIM][BF <sub>4</sub> ]	RT	8050	40
19	[EMIM][BF <sub>4</sub> ]	RT	6670	40
20	[BMIM][BF <sub>4</sub> ]	RT	3370	40
21	[HMIM][BF <sub>4</sub> ]	RT	2880	40
22	[OMIM][BF <sub>4</sub> ]	RT	1910	40
23	[BMIM][PF <sub>6</sub> ]	RT	3270	40
24	[MMIM][Tf <sub>2</sub> N]	RT	1340	40
25	[EMIM][Tf <sub>2</sub> N]	RT	1180	40
26	[BMIM][Tf <sub>2</sub> N]	RT	950	40
27	[HMIM][Tf <sub>2</sub> N]	RT	760	40
28	[OMIM][Tf <sub>2</sub> N]	RT	670	40
29	[BzMIM][Tf <sub>2</sub> N]	RT	1410	40
30	[BMIM][PF <sub>6</sub> ]	RT	55.2	41
31	[BMIM][PF <sub>6</sub> ]	100	56.0	41
32	[BMIM][BF <sub>4</sub> ]	RT	1726	39
33	[BMIM][BF <sub>4</sub> ]	50	1765	39
34	[BMIM][BF <sub>4</sub> ]	70	1775	39

found, leading to a small decrease in CO solubility at higher temperatures.



**Figure 1.** Effect of the alkyl chain length in [RMIM][X] (X = BF<sub>4</sub><sup>-</sup> and Tf<sub>2</sub>N<sup>-</sup>) ionic liquids on CO gas solubility expressed by Henry coefficients. Data reproduced from ref 40.

**Table 3. Alkene Solubility in Ionic Liquids Expressed by the Henry Coefficient (at 1 Bar)**

entry	alkene	ionic liquid	$T$ (°C)	Henry coefficient, $k_H$ (bar)	ref
35	ethene	[BMIM][PF <sub>6</sub> ]	10	142 ± 14	36
36		[BMIM][PF <sub>6</sub> ]	25	173 ± 17	36
37		[BMIM][PF <sub>6</sub> ]	50	221 ± 22	36
38		[EMIM][Tf <sub>2</sub> N]	30	148 ± 2.8	42, 43
39		[EMIM][Tf <sub>2</sub> N]	40	151 ± 2.8	42, 43
40		[BMIM][BF <sub>4</sub> ]	40	118 ± 7	42, 43
41		[BMIM][PF <sub>6</sub> ]	40	126 ± 8	42, 43
42	propene	[EMIM][Tf <sub>2</sub> N]	30	263 ± 24	42, 43
43		[EMIM][Tf <sub>2</sub> N]	40	243 ± 21	42, 43
44		[BMIM][BF <sub>4</sub> ]	40	187 ± 23	42, 43
45		[BMIM][PF <sub>6</sub> ]	40	189 ± 23	42, 43
46	1-butene	[EMIM][Tf <sub>2</sub> N]	30	37.0 ± 0.5	42, 43
47		[EMIM][Tf <sub>2</sub> N]	40	37.1 ± 0.5	42, 43
48		[EMIM][Tf <sub>2</sub> N]	40	44.3 ± 1.4	42, 43
49		[EMIM][Tf <sub>2</sub> N]	40	44.4 ± 1.4	42, 43
50		[BMIM][BF <sub>4</sub> ]	40	88.2 ± 2.9	42, 43
51		[BMIM][PF <sub>6</sub> ]	40	87.8 ± 2.8	42, 43
52		[BMIM][PF <sub>6</sub> ]	40	74.0 ± 3.5	42, 43
53		[BMIM][Tf <sub>2</sub> N]	7	74.2 ± 3.5	44
54		[BMIM][Tf <sub>2</sub> N]	27	15.3	44
55		[BMIM][Tf <sub>2</sub> N]	47	23.0	44
56		[BMIM][Tf <sub>2</sub> N]	67	33.6	44
57		[EMIM][Tf <sub>2</sub> N]	40	45.8	44
58		[EMIM][Tf <sub>2</sub> N]	40	22.2 ± 0.4	42, 43
59		[EMIM][Tf <sub>2</sub> N]	40	22.2 ± 0.4	42, 43
60		[BMIM][BF <sub>4</sub> ]	40	54.4 ± 1.1	42, 43
61		[BMIM][PF <sub>6</sub> ]	40	55.6 ± 1.2	42, 43
62		[BMIM][PF <sub>6</sub> ]	40	40.5 ± 1.1	42, 43
63		[BMIM][PF <sub>6</sub> ]	40	40.4 ± 1.0	42, 43
64		[BMIM][Tf <sub>2</sub> N]	7	6.5	44
65		[BMIM][Tf <sub>2</sub> N]	27	10.5	44
66		[BMIM][Tf <sub>2</sub> N]	47	16.7	44
67		[BMIM][Tf <sub>2</sub> N]	67	26.0	44
68		[EMIM][Tf <sub>2</sub> N]	40	8.53 ± 0.07	42, 43
69		[EMIM][Tf <sub>2</sub> N]	40	8.54 ± 0.07	42, 43
70		[BMIM][BF <sub>4</sub> ]	40	n/a	42, 43
71		[BMIM][PF <sub>6</sub> ]	40	13.4 ± 0.2	42, 43
72		[BMIM][PF <sub>6</sub> ]	40	13.3 ± 0.2	42, 43

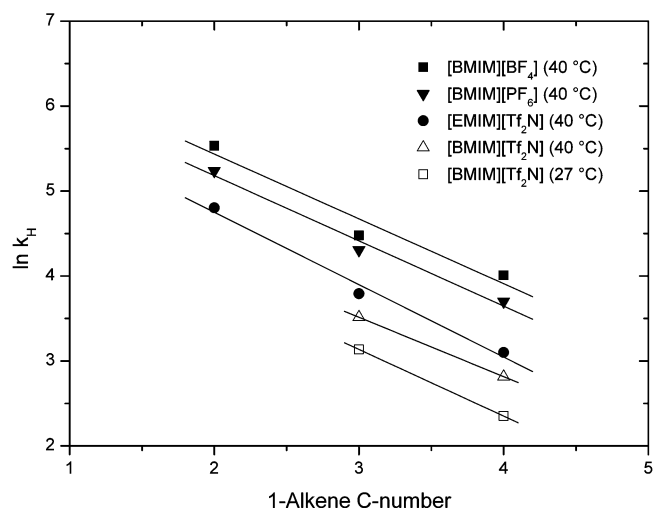
CO solubility in [BMIM][PF<sub>6</sub>] was also measured by Maurer et al. in 2005 using a high-pressure view cell that allowed the determination of the solubility pressure at equilibrium and thus the Henry constant (on the molality scale) (entries 30 and 31).<sup>41</sup> In good agreement with the previous results by Dyson et al.,<sup>40</sup> no significant temperature dependence was observed.

## 2.2. Ethene, Propene, and 1-Butene Solubility

In addition to the pioneering work by Brennecke,<sup>36</sup> the solubility of short chain alkenes in ionic liquids has recently been determined independently by Noble et al.<sup>42,43</sup> and Outcalt et al.<sup>44</sup> using pressure decay inside a sealed vessel to calculate the alkene solubility (Table 3).

Noble and co-workers reported values for ethene in [BMIM][PF<sub>6</sub>], which were in good agreement with the data from Brennecke et al.<sup>36</sup> (compare entries 35–37 with entry 41).<sup>42</sup> However, in the ionic liquid [EMIM][Tf<sub>2</sub>N], the solubility of ethene increased with increasing temperature (entries 38 and 39),<sup>43</sup> in contrast to the case in [BMIM][PF<sub>6</sub>], for which Brennecke reported a decrease in solubility.<sup>36</sup>

Noble et al. also reported a better solubility in ionic liquids at 40 °C when going from ethene to propene and 1-butene (entries 39–41, 43–45, and 50–52).<sup>42</sup> This trend was also observed by Outcalt et al. for propene and 1-butene in [BMIM][Tf<sub>2</sub>N] at temperatures between 7 and 67 °C (entries



**Figure 2.** Alkene solubility in different [RMIM][X] (R = ethyl and butyl; X = BF<sub>4</sub><sup>-</sup>, PF<sub>6</sub><sup>-</sup>, and Tf<sub>2</sub>N<sup>-</sup>) ionic liquids expressed with Henry coefficients (closed symbols, refs 42 and 43; open symbols, ref 44).

46–49 and 53–56).<sup>44</sup> Interestingly, in [BMIM][Tf<sub>2</sub>N], the alkene solubility decreased with increasing temperature, whereas it increased in the ionic liquid [EMIM][Tf<sub>2</sub>N].

For the four ionic liquids studied, the solubility of the alkene gases increased with increasing carbon number with a similar solubility behavior. Hence, a plot of  $\ln k_H$  against the carbon number of the alkenes revealed a linear decline in  $\ln k_H$  with increasing chain length, as shown in Figure 2. The average slope of all fitted curves, regardless of ionic liquid type, was found to be  $-0.77 \pm 0.05$ .

Overall, the compiled gas solubility data in Tables 1–3 might indicate that ionic liquid biphasic hydroformylation reactions are mass transport limited. Especially the low hydrogen solubility should result in slow reaction rates. However, in many cases, an accelerating effect of the ionic liquid has been reported. This will be further discussed in sections 4.1 and 5.2.

## 2.3. Alcohol and Aldehyde Solubility

Aldehydes and alcohols are the typical hydroformylation products, with the latter being produced from the aldehydes by hydrogenation in a consecutive reaction. Aldol condensation of the formed aldehydes and alcohols results in higher alcohols with twice the carbon number. These so-called heavy boiling products (heavies) are an undesired byproduct in most hydroformylation processes.<sup>45</sup> All products and byproducts have a higher polarity compared to the alkene substrate and can therefore likely be accumulated within the ionic liquid phase.<sup>46</sup> The literature data on short chain alcohol and aldehyde solubility in selected ionic liquids, most commonly used for hydroformylation experiments, have been summarized in Table 4 in terms of their activity coefficients at infinite dilution  $\gamma_i^\infty$ .

In hydrophilic [EMIM][C<sub>2</sub>H<sub>5</sub>OSO<sub>3</sub>], the activity coefficients of both alcohols and aldehydes increased significantly with increasing C-number of the solute (entries 60–63).<sup>47</sup> The same trend was observed for alcohol solubility in the more hydrophobic ionic liquids [EMIM][Tf<sub>2</sub>N] (entries 64–67), [BMIM][Tf<sub>2</sub>N] (entries 68–71), and [HMIM][Tf<sub>2</sub>N] (entries 72–76).<sup>48–52</sup> With increasing alkyl chain length R on the cation [RMIM]<sup>+</sup>, the activity coefficients decreased

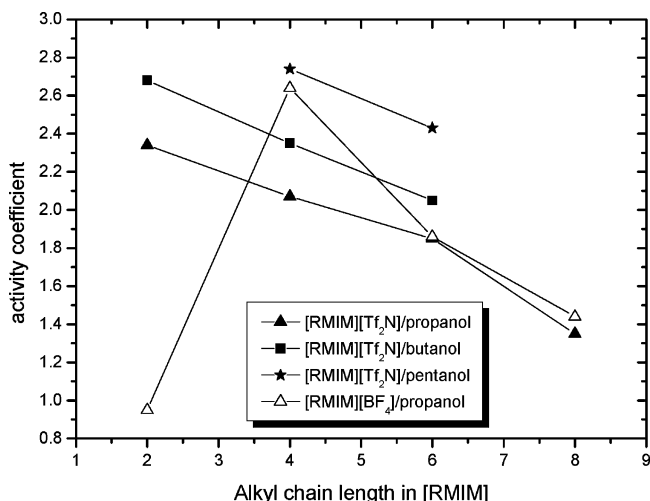
**Table 4. Alcohol and Aldehyde Solubility in Selected Ionic Liquids at 323 K Expressed by the Infinite Dilution Coefficient  $\gamma_i^\infty$**

entry	ionic liquid	alcohol		aldehyde			
			$\gamma_i^\infty$	ref	$\gamma_i^\infty$	ref	
60	[EMIM][C <sub>2</sub> H <sub>5</sub> OSO <sub>3</sub> ]	1-propanol	1.22	47	propanal	2.00	47
61		1-butanol	1.69	47	1-butanal	3.47	47
62		1-pentanol	2.74	47	1-pentanal	5.37	47
63		1-hexanol	4.20	47	1-hexanal	11.22	47
64	[EMIM][Tf <sub>2</sub> N]	1-propanol	1.90	48			
65		1-propanol	2.02	49			
66		1-butanol	2.68	48			
67		1-pentanol	3.78	48			
68	[BMIM][Tf <sub>2</sub> N]	1-propanol	2.07	50	propanal	0.49	50
69		1-butanol	2.35	50	1-butanal	0.68	50
70		1-pentanol	2.74	50	1-pentanal	1.34	50
71		1-hexanol	3.47	50	1-hexanal	1.51	50
72	[HMIM][Tf <sub>2</sub> N]	1-propanol	1.85	51	propanal	0.45	51
73		1-propanol	1.57	52			
74		1-butanol	2.05	51	1-butanal	0.58	51
75		1-pentanol	2.43	51	1-pentanal	1.08	51
76		1-hexanol	2.92	51	1-hexanal	1.19	51
77	[OMIM][Tf <sub>2</sub> N]	1-propanol	1.35	52			
78	[EMIM][BF <sub>4</sub> ]	1-propanol	0.95	53			
79	[BMIM][BF <sub>4</sub> ]	1-propanol	2.64	53			
80		1-propanol	2.23	54			
81		1-butanol	3.30	54			
82		1-pentanol	5.15	54			
83	[HMIM][BF <sub>4</sub> ]	1-propanol	1.86	53			
84	[OMIM][BF <sub>4</sub> ]	1-propanol	1.44	53			

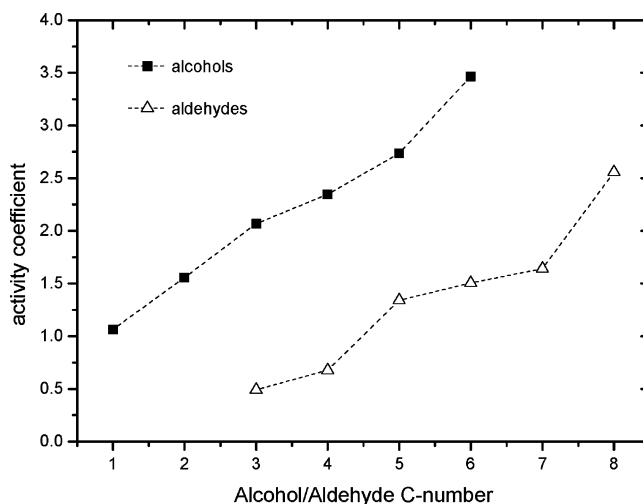
for all alcohols, as shown in Figure 3. In [RMIM][BF<sub>4</sub>] ionic liquids, a similar behavior of decreasing activity coefficients with increasing alkyl chain was observed, with the exception of [EMIM][BF<sub>4</sub>], having the lowest activity coefficient in the series (entries 79–84 and Figure 3).<sup>53,54</sup>

Activity coefficient data for the corresponding aldehydes are compiled in Table 3. They follow a similar trend as observed for the alcohols, as depicted in Figure 4.

A clear trend was observed of increasing activity coefficients (and thus solubility) with increasing C-number of the substrate. This behavior indicates that the byproducts of the hydroformylation are better soluble in the ionic liquid than the desired aldehyde products. In the case of aldol condensation, the resulting alcohols should be more soluble in the ionic liquid phase by orders of magnitude. In such a scenario, it will become important to find ways to remove



**Figure 3.** Activity coefficients of short chain 1-alcohols in [RMIM]-[Tf<sub>2</sub>N] and [RMIM][BF<sub>4</sub>] ionic liquids as a function of alkyl chain length R at 323 K. Data reproduced from refs 47–54.



**Figure 4.** Activity coefficients of short chain 1-alcohols and 1-aldehydes in the ionic liquid [BMIM][Tf<sub>2</sub>N] at 353 K. Data reproduced from ref 50.

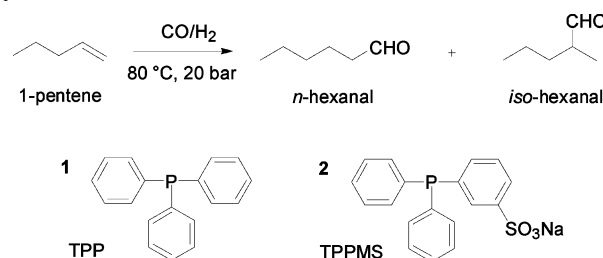
these heavies from the ionic liquid phase; otherwise, a dilution of the catalyst concentration will result in lower reaction rates. Furthermore, these heavies can cause catalyst metal leaching from the ionic liquid phase into the organic phase.

### 3. Biphasic Hydroformylation with Ionic Liquids

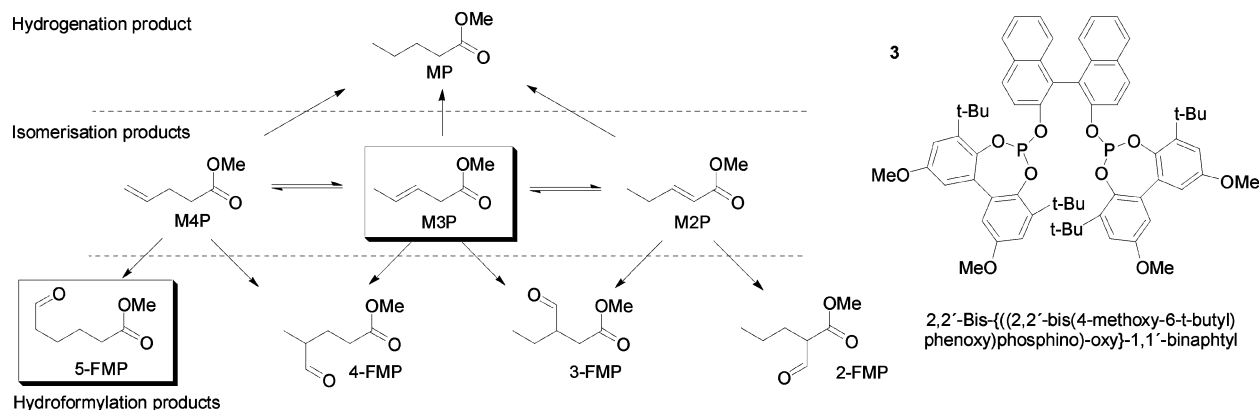
#### 3.1. Ionic Liquid Progression

The first investigations of the rhodium-catalyzed hydroformylation in room temperature ionic liquids were published by Chauvin et al. in 1995.<sup>20</sup> Here, reaction of 1-pentene with the catalyst system Rh(acac)(CO)<sub>2</sub>/triarylphosphine was carried out in a biphasic reaction mode using [BMIM][PF<sub>6</sub>] as the ionic liquid, according to Scheme 1.

**Scheme 1. Hydroformylation of 1-Pentene with Rh(acac)(CO)<sub>2</sub>/Triarylphosphine Catalyst Systems Studied by Chauvin<sup>20</sup>**



In this study, it was not possible to combine high activity, complete retention of the catalyst in the ionic liquid, and high selectivity for the desired linear hydroformylation product, with any of the well-established ligands tested. The use of TPP (**1**) resulted in significant leaching of the Rh catalyst into the product phase, thus resulting in catalyst activity in both phases. The catalyst leaching could be suppressed by the application of the same sulfonated triarylphosphine ligands [e.g., TPPMS (**2**)] that are used with great success in aqueous biphasic catalysis (e.g., the RCH/RP process<sup>7</sup>). Surprisingly, these ligands were found to cause major deactivation when applied in an ionic liquid medium [TOF = 59 h<sup>-1</sup> with TPPMS (**2**) compared to 333 h<sup>-1</sup> with TPP (**1**)]. Moreover, all of the established ligands showed

**Scheme 2. Reaction Routes to Hydrogenation-, Isomerization-, and Hydroformylation Products of Methyl-3-pentenoate under Syngas**

**Table 5. Rh-Catalyzed Hydroformylation<sup>a</sup> of M3P in Toluene and the Ionic Liquid [BMIM][PF<sub>6</sub>]<sup>55</sup>**

entry	solvent	ligand	TOF (h <sup>-1</sup> )	selectivity (%)					<i>n</i> / <i>iso</i> ratio
				MP	2-FMP	3-FMP	4-FMP	5-FMP	
85	toluene	<b>1</b>	83	4	9	42	39	3	<0.1
86	toluene	<b>3</b>	89	12	0	12	25	50	1.3
87	[BMIM][PF <sub>6</sub> ]	<b>1</b>	107	7	7	37	38	10	0.1
88	[BMIM][PF <sub>6</sub> ]	<b>3</b>	180	5	0	17	29	47	1.0

<sup>a</sup> Reaction conditions:  $p(\text{H}_2/\text{CO} = 1:1) = 10$  bar,  $T = 110$  °C,  $t = 3$  h, Rh(acac)(CO)<sub>2</sub> precursor, L/Rh = 4, M3P/Rh = 3000.

poor selectivity for the desired linear hydroformylation product (*n*-hexanal between 50 and 80%).

In 1999, Keim et al. used the ionic liquid [BMIM][PF<sub>6</sub>] and two different rhodium catalysts to study the hydroformylation of methyl-3-pentenoate (M3P), which is a model feedstock for fatty esters and an important intermediate in the synthesis of nylon or polyesters.<sup>55</sup> Controlling the reaction selectivity toward linear aldehyde was important here, since M3P can undergo isomerization as well as hydrogenation, leading to unwanted side products, as depicted in Scheme 2.

Recycling experiments were carried out in a batch autoclave with distillative product removal at the end of the reaction. Table 5 summarizes the results obtained for two ligand modified rhodium complexes in biphasic ionic liquid systems and in organic solution (i.e., homogeneous).

The regioselectivity was not influenced by the solvent but solely by the type of ligand. Using the bulky phosphite ligand **3** enhanced the isomerization tendency of catalysts and resulted in the increased formation of the desired 5-FMP. Recycling experiments with TPP (**1**) as ligand resulted in deactivation of the catalyst after the first cycle (in the case of organic solvent) and the fourth cycle (in the case of [BMIM][PF<sub>6</sub>]). With the thermally more stable ligand **3**, the catalyst deactivated after the third cycle when using organic solvents but largely retained its activity in [BMIM][PF<sub>6</sub>], resulting in TONs of 6640 after ten cycles, as shown in Table 6.

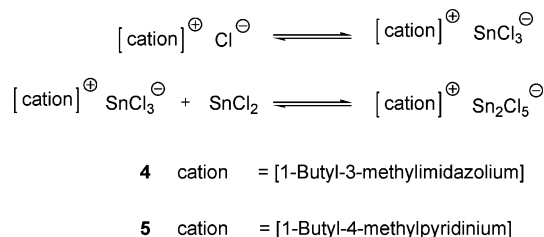
Methyl-3-pentenoate (M3P) was also hydroformylated using Pt(TPP)<sub>2</sub>Cl<sub>2</sub> catalyst complexes in Lewis acidic chlorostannate ionic liquids by Wasserscheid and Waffenschmidt in 2000.<sup>56</sup> The Lewis acidity of the ionic liquid was adjusted by the chloride/tin(II) chloride ratio, as depicted in Scheme 3, and could be correlated with the chemical shift of the <sup>119</sup>Sn NMR signal in the melts. Increasing the amount of SnCl<sub>2</sub> resulted in a significant upfield shift of the <sup>119</sup>Sn signal.

Besides reaction of methyl-3-pentenoate, hydroformylation of 1-octene was also investigated in these chlorostannate

**Table 6. Recycling Experiments<sup>a</sup> with Rh-3 Catalyst in the M3P Hydroformylation<sup>55</sup>**

entry	cycle	CH <sub>2</sub> Cl <sub>2</sub>		toluene		[BMIM][PF <sub>6</sub> ]	
		TOF (h <sup>-1</sup> )	TON	TOF (h <sup>-1</sup> )	TON	TOF (h <sup>-1</sup> )	TON
89	0	134	630	91	455	149	745
90	1	42	255	25	125	159	795
91	2	19	95	10	50	92	460
92	3	0	0	0	0	149	745
93	4–10	0	0	0	0	80–150	3575
Σ <sub>TON</sub>		980		630		6640	

<sup>a</sup> Reaction conditions:  $p(\text{H}_2/\text{CO} = 1:1) = 30$  bar,  $T = 110$  °C,  $t = 5$  h, Rh(acac)(CO)<sub>2</sub> precursor, **3**/Rh = 4, M3P/Rh = 1300.

**Scheme 3. Lewis Acidic Chlorostannate Ionic Liquid Systems**


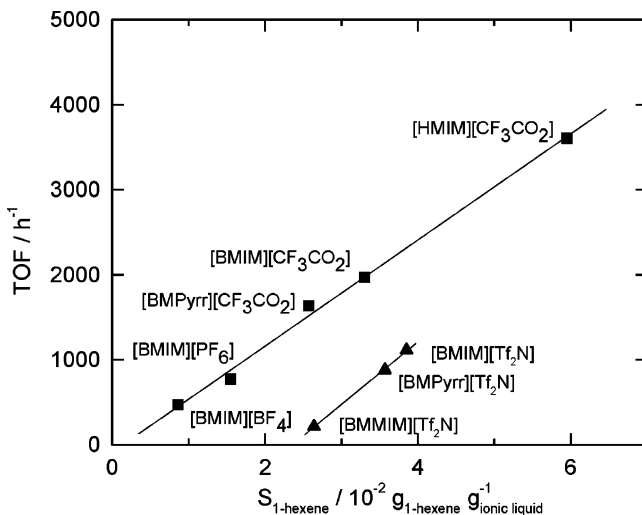
ionic liquids and compared to reactions using CH<sub>2</sub>Cl<sub>2</sub> as solvent. In Table 7, the results are compiled.

For M3P, the overall activity of the Pt catalyst was significantly higher in the chlorostannate ionic liquids than in the organic solvent CH<sub>2</sub>Cl<sub>2</sub> (entries 94–96). Using 1-octene as substrate, the Pt catalyst exhibited similar activities in both solvents (entries 97–99). The selectivity toward *n*-nonanal in the ionic liquids was comparable to that for the organic monophasic systems as well. However, as for the case of M3P, the hydrogenation tendency for 1-octene of the platinum complex was significantly higher in the ionic liquids than in CH<sub>2</sub>Cl<sub>2</sub>, which was attributed to a higher hydrogen solubility compared to CO.

**Table 7. Pt-1-Catalyzed Hydroformylation<sup>a</sup> of M3P and 1-Octene in Chlorostannate Ionic Liquids<sup>56</sup>**

entry	substrate	solvent	conversion (%)	TOF (h <sup>-1</sup> )	S <sub>ald</sub> (%)	S <sub>hyd</sub> (%)
94 <sup>b</sup>	M3P	5/SnCl <sub>2</sub>	5.4	31	56.5	9.6
95 <sup>b</sup>	M3P	4/SnCl <sub>2</sub>	6.3	37	56.5	9.8
96 <sup>b</sup>	M3P	CH <sub>2</sub> Cl <sub>2</sub>	1.5	9	44.4	4.6
97 <sup>c</sup>	1-octene	5/SnCl <sub>2</sub>	19.7	103	96.0	29.4
98 <sup>c</sup>	1-octene	4/SnCl <sub>2</sub>	22.3	126	95.0	41.7
99 <sup>c</sup>	1-octene	CH <sub>2</sub> Cl <sub>2</sub>	25.7	140	98.3	9.4

<sup>a</sup> Reaction conditions:  $T = 120$  °C,  $t = 2$  h, Pt(1)<sub>2</sub>Cl<sub>2</sub> 0.02 mmol, 1/Pt = 5 (entries 94, 95, 97, and 98), substrate/Pt = 1000, 5 mL of solvent,  $X(\text{SnCl}_2) = 0.51$  (entries 94, 95, 97, and 98). <sup>b</sup>  $p(\text{H}_2/\text{CO}) = 1:1 = 50$  bar. <sup>c</sup>  $p(\text{H}_2/\text{CO}) = 1:1 = 90$  bar.

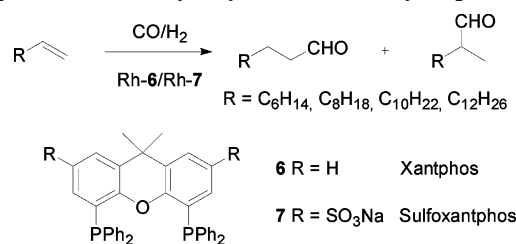


**Figure 5.** Turn-over-frequency (at 25% conversion) for 1-hexene hydroformylation as a function of 1-hexene solubility in the ionic liquids. Data reproduced from ref 57 (Reaction conditions:  $p(\text{H}_2/\text{CO}) = 1:1 = 20$  bar,  $T = 80$  °C, Rh(acac)(CO)<sub>2</sub> 0.075 mmol, 2/Rh = 4, 1-hexene/Rh = 800).

The first systematic approach to investigating ionic liquid structure influences on hydroformylation was reported by Olivier-Bourbigou et al. in 2001, using a range of ionic liquids with variation in both cations (e.g., 1,3-dialkylimidazolium, 1,2,3-trialkylimidazolium, and *N,N*-dialkylpyrrolidinium), and anions (e.g., BF<sub>4</sub><sup>-</sup>, PF<sub>6</sub><sup>-</sup>, CF<sub>3</sub>CO<sub>2</sub><sup>-</sup>, CF<sub>3</sub>SO<sub>3</sub><sup>-</sup>, TfO<sup>-</sup>, and NTf<sub>2</sub><sup>-</sup>).<sup>57</sup> The solubility of 1-hexene in the different ionic liquids was measured and found to be linearly correlated with the activity of a Rh-TPPMS catalyst, as shown in Figure 5, with the 1-hexene solubility plotted on the x-axis and the observed activity (expressed as TOF) on the y-axis.

In addition, the 1-hexene solubility was found to increase significantly with increasing alkyl chain length of the cation for a given anion (e.g., CF<sub>3</sub>CO<sub>2</sub><sup>-</sup>), while only minor effects were observed when changing the cation from [BMIM]<sup>+</sup> to [BMPyr]<sup>+</sup> (e.g., for the anions CF<sub>3</sub>CO<sub>2</sub><sup>-</sup> and Tf<sub>2</sub>N<sup>-</sup>). Moreover, methylation in the 2-position on the imidazolium cation seemed to decrease the substrate solubility. For BMIM-based ionic liquids, 1-hexene solubility was further found to increase in the following order: BF<sub>4</sub><sup>-</sup> < PF<sub>6</sub><sup>-</sup> < TfO<sup>-</sup> < CF<sub>3</sub>CO<sub>2</sub><sup>-</sup> < Tf<sub>2</sub>N<sup>-</sup>. Reaction selectivity was high, around 97%, in all cases, and no recycling experiments were reported.

Dupont and co-workers studied the influence of different ionic liquids on the hydroformylation of long chain alkenes in 2001.<sup>58</sup> Ligand modification of the rhodium catalyst was

**Scheme 4. Hydroformylation of 1-Octene, 1-Decene, 1-Dodecene, and 1-Tetradecene with Rh(acac)(CO)<sub>2</sub>/Xantphos-Based Catalyst Systems Studied by Dupont et al.<sup>58</sup>****Table 8. Rh-7-Catalyzed Hydroformylation<sup>a</sup> of 1-Octene in [BMIM][PF<sub>6</sub>]<sup>58</sup>**

entry	$p$ (bar)	$T$ (°C)	conversion (%)	TOF (h <sup>-1</sup> )	$n$ -nonanal (%)	S <sub>iso</sub> (%)
100	5	80	61	25	82	37
101	15	80	90	37	83	15
102	25	80	66	28	76	22
103	35	80	60	23	72	21
104	15	60	5	2	72	21
105	15	100	77	32	93	21
106	15	120	86	36	90	25
107	15	140	94	39	88	29

<sup>a</sup> Reaction conditions:  $t = 24$  h, Rh(acac)(CO)<sub>2</sub> 0.02 mmol, 7/Rh = 4, 1-octene/Rh = 1000, 3 mL of [BMIM][PF<sub>6</sub>].

achieved by use of chelating xantphos (**6**) and sulfoxantphos (**7**) ligands, shown in Scheme 4.

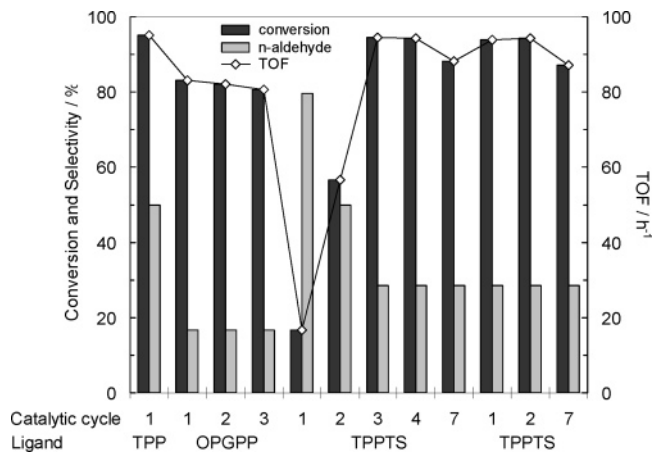
The xantphos ligand showed high activity (TOF = 245 h<sup>-1</sup>) in the first run of 1-octene hydroformylation in [BMIM][PF<sub>6</sub>]. However, a large amount of the rhodium leached into the organic phase and the conversion dropped from 99% to 60% upon recycling. The sulfoxantphos modified rhodium complex (ligand to rhodium ratio, i.e., L/Rh = 1) was recycled up to three times in [BMIM][PF<sub>6</sub>] without loss of activity. Under these conditions, a low selectivity of 65.5% toward the linear nonanal was obtained. When the L/Rh ratio was adjusted to 5, the selectivity increased to 80% *n*-nonanal and remained constant over four recycles. During the course of this recycling, an incubation period was observed, and the catalyst reached the highest activity only after the second cycle. Table 8 summarizes the results obtained from experiments at different temperatures and syngas pressures.

Surprisingly, the catalytic activity was found to decrease when the syngas pressure was increased to above 15 bar using [BMIM][PF<sub>6</sub>] at 80 °C. In the temperature range 80–140 °C, the reaction was further found to be limited by mass transport from the gas into the liquid phase, indicated by an effective activation energy of 6.3 kJ mol<sup>-1</sup>, with the level of 1-octene isomerization remaining high, above 15%. By comparing different ionic liquids systems such as pure [BMIM][PF<sub>6</sub>] (hydrophobic), water-saturated [BMIM][PF<sub>6</sub>], [BMIM][PF<sub>6</sub>] with toluene cosolvent, and pure [BMIM][BF<sub>4</sub>] (hydrophilic), it was further found that lower selectivity toward linear aldehyde was obtained with the more hydrophilic or water-containing solvent systems. Hence, the highest linear selectivity was observed in pure [BMIM][PF<sub>6</sub>] with 93% *n*-nonanal, while 1-decene resulted in almost exclusive formation of *n*-undecanal with up to 98.4% linearity. Suspicion should, however, be taken when elucidating the reported selectivity order, considering the likelihood for particular [PF<sub>6</sub>]<sup>-</sup> ionic liquid anion hydrolysis with possible catalyst degradation, as also earlier emphasized in this review.

In 2002 Wasserscheid et al. reported the synthesis and use of the halogen-free ionic liquid [BMIM][*n*-C<sub>8</sub>H<sub>17</sub>OSO<sub>3</sub>] for

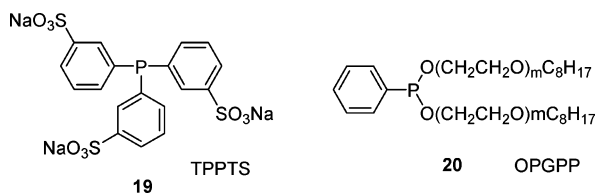






**Figure 6.** Recycling results obtained from Rh-catalyzed hydroformylation of 1-tetradecene in an ionic liquid **18**/heptane system. Reproduced based on data from ref 63. (Reaction conditions:  $p(\text{H}_2/\text{CO}) = 1:1 = 50$  bar,  $T = 105$  °C,  $t = 10$  h,  $\text{RhCl}_3$  precursor, ligands/Rh = 15, 1-tetradecene/Rh = 1000, 2.0 g of **18**, 1.0 mL of tetradecene, 0.2 mL of *n*-heptane. The last results with the ligand TPPTS (**19**) were obtained after 20 h of preformation of active catalyst.)

**Scheme 8. Structures of Sodium Tris(*m*-sulfonatophenyl)-phosphine (TPPTS) Ligand and Octylpolyethylene-glycolphenylphosphite (OPGPP) Ligand<sup>63</sup>**

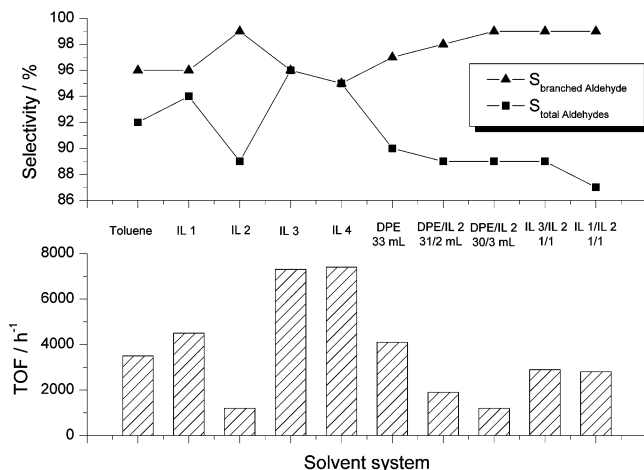


phase and suppress leaching without loss of activity. The selectivity was, however, very low in all cases, with only up to 29% *n*-pentadecanal being formed.

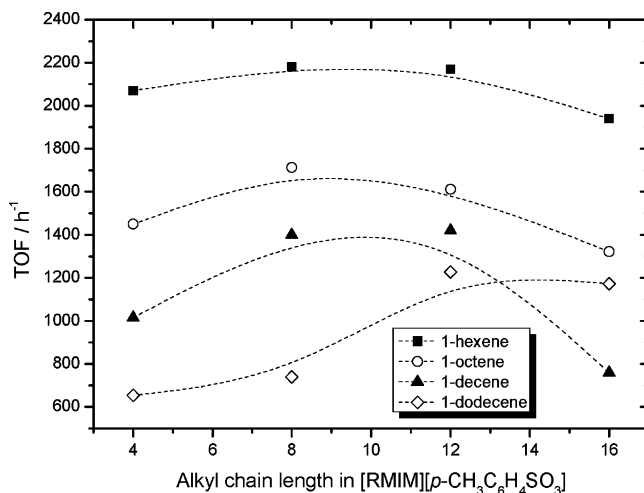
In a recent paper, Williams and co-workers investigated the influence of different ionic liquids and mixtures thereof on the activity and selectivity of the hydroformylation of vinyl acetate to yield mainly branched aldehydes.<sup>64</sup> The ionic liquids tested were [BMIM][Tf<sub>2</sub>N] (IL 1), [N(C<sub>8</sub>H<sub>17</sub>)<sub>3</sub>CH<sub>3</sub>][Tf<sub>2</sub>N] (IL 2), [N(C<sub>6</sub>H<sub>5</sub>)(C<sub>2</sub>H<sub>5</sub>)][Tf<sub>2</sub>N] (IL 3), and [BPyrr][Tf<sub>2</sub>N] (IL 4). As can be seen from Figure 7, the type of ionic liquid enhanced the activity significantly, with IL 3 and IL 4 exceeding the homogeneous toluene solvent by a factor of 2.

In all systems, the selectivity toward aldehyde formation was high. The highest selectivity for branched aldehydes was obtained when using [N(C<sub>8</sub>H<sub>17</sub>)<sub>3</sub>CH<sub>3</sub>][Tf<sub>2</sub>N] (IL 2). The positive effect of the ionic liquid on the selectivity was confirmed by mixing a small amount with diphenyl ether (DPE). With decreasing amounts of ionic liquid, the activity could be increased; however, the selectivity decreased. Mixing of different ionic liquids (IL 1 and 2, IL 3 and 2) resulted in a 2.5-fold increase in activity (TOF 1200 h<sup>-1</sup> compared to 2800 and 2900 h<sup>-1</sup>, respectively) while at the same time the selectivity increased as well. These mixing results indicate the possibility to blend ionic liquid systems to combine beneficial properties for catalysis.

The influence of the cation and anion of different ionic liquids has been reported by Lin et al. for the rhodium-catalyzed hydroformylation of 1-alkenes using TPPTS (**19**) and BISBIS (sodium salt of sulfonated 2,2'-bis(diphenylphosphinomethyl)-1,1'-biphenyl) ligands.<sup>65</sup> In 1-hexene



**Figure 7.** Influence of solvent nature on activity (TOF) and selectivity in the hydroformylation of vinyl acetate. Reproduced with data from ref 64. (Reaction conditions:  $p(\text{H}_2/\text{CO}) = 1:1 = 20$  bar,  $T = 85$  °C, ligand/Rh = 3, ligand = tris(2,4-di-*tert*-butylphenyl)phosphite, 1 mM  $\text{Rh}(\text{CO})_2(\text{acac})$ , 7 M vinyl acetate or 2 mM when using DPE as solvent.)



**Figure 8.** Influence of cation alkyl chain length on 1-alkene hydroformylation activity expressed as TOF. Reproduced based on data from ref 65. (Reaction conditions:  $p(\text{H}_2/\text{CO}) = 1:1 = 30$  bar,  $T = 100$  °C,  $t = 1$  h, 0.01 mmol  $\text{Rh}(\text{CO})_2(\text{acac})$ , **19**/Rh = 10, 1 mL of ionic liquid, 3 mL of 1-alkene.)

hydroformylation, a significant enhancement in catalyst activity was observed when replacing [BMIM][PF<sub>6</sub>] (TOF = 54 h<sup>-1</sup>) with the ionic liquids [BMIM][BF<sub>4</sub>] (TOF = 1748 h<sup>-1</sup>) and [BMIM][*p*-CH<sub>3</sub>C<sub>6</sub>H<sub>4</sub>SO<sub>3</sub>] (TOF = 2070 h<sup>-1</sup>), which was attributed to the better solubility of the TPPTS ligand in these ionic liquids. Changing the alkyl chain length of the imidazolium cation stepwise from C4 to C8 to C12 to C16 resulted in no significant improvement in 1-hexene hydroformylation, as shown in Figure 8.

However, when using longer chain 1-alkenes as substrate, the cation chain length influenced the activity. Figure 8 shows the change in TOF for 1-hexene, 1-octene, 1-decene, and 1-dodecene hydroformylation. The longer the alkene, the stronger the observed activity change with increasing alkyl chain length. This effect was attributed to the interplay between improved alkene solubility and lowered ligand solubility for increasing alkyl chains. The selectivity was less affected by the change in ionic liquid in all experiments. Recycling experiments in the 1-hexene hydroformylation indicated good stability of the catalyst in the ionic liquid

**Table 10. Catalyst Recycling in Rh-19-Catalyzed 1-Hexene Hydroformylation<sup>a</sup> Using the Ionic Liquid [BMIM][p-CH<sub>3</sub>C<sub>6</sub>H<sub>4</sub>SO<sub>3</sub>]<sup>65</sup>**

entry	run	conversion (%)	S <sub>ald</sub> (%)	n-pentanal (%)	Rh-leaching (wt %)
112	1	95.0	93.8	75.0	0.061
113	2	92.6	92.6	75.0	
114	3	96.2	91.7	74.4	0.052
115	4	97.7	91.0	73.7	
116	5	99.4	90.6	73.7	0.024
117	6	99.6	90.5	73.0	
118	7	99.8	90.2	72.2	
119	8	99.6	86.3	72.2	
120	9	99.8	79.9	71.4	
121	10 <sup>b</sup>	98.5	93.6	73.0	

<sup>a</sup> Reaction conditions:  $p(\text{H}_2/\text{CO} = 1:1) = 30$  bar,  $T = 100$  °C,  $t = 1$  h, 0.01 mmol of Rh(CO)<sub>2</sub>acac, **19**/Rh = 12, 3 mL of 1-alkene, 1 mL of [BMIM][p-CH<sub>3</sub>C<sub>6</sub>H<sub>4</sub>SO<sub>3</sub>]. <sup>b</sup> 0.04 mmol of TPPTS (**19**) ligand was added.

[BMIM][p-CH<sub>3</sub>C<sub>6</sub>H<sub>4</sub>SO<sub>3</sub>] with no significant loss in activity and selectivity during ten consecutive runs. The recycling results are compiled in Table 10.

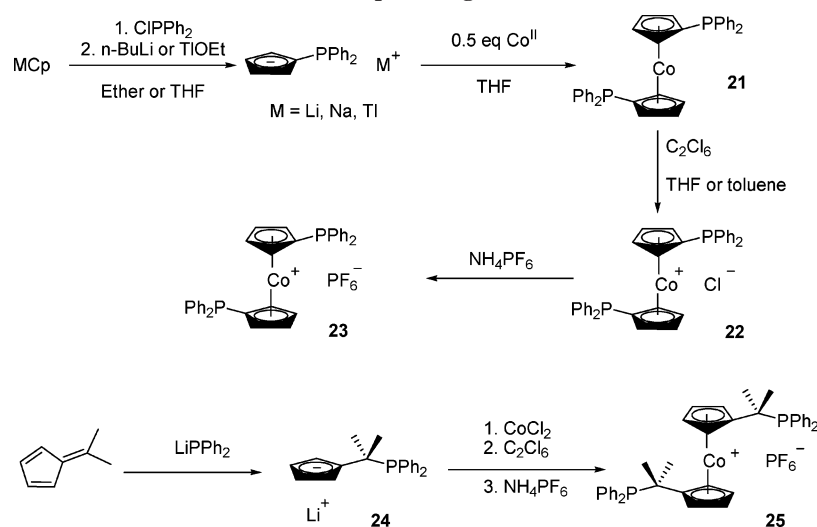
After the ninth run, small amounts of fresh TPPTS were added to the solution in order to compensate for oxidized ligand and thus suppress formation of unmodified rhodium species. As a result, the initial activity and selectivity could be recovered in the tenth run.

## 3.2. Progression in Ligand Design

### 3.2.1. Achiral Ligands

Although early work of Chauvin et al.<sup>20</sup> showed the potential of ionic liquids as alternative solvents for biphasic catalysis, the overall results obtained with the rhodium catalyst were poor. The use of TPP (**1**) as ligand led to acceptable rates but high Rh leaching into the organic phase, while the TPPMS ligand **2** enabled catalyst to retain in the ionic liquid phase but decreased activity significantly. Moreover, all tested ligands induced low selectivity to the desired linear aldehyde. Consequently, novel tailor-made ligands have been developed for biphasic ionic liquid hydroformylation, combining high activity and high selectivity with good durability.

In one of the first examples applying rational ligand design, Brasse et al. synthesized ionic phosphine ligands with a cobaltocenium backbone according to Scheme 9.<sup>66</sup>

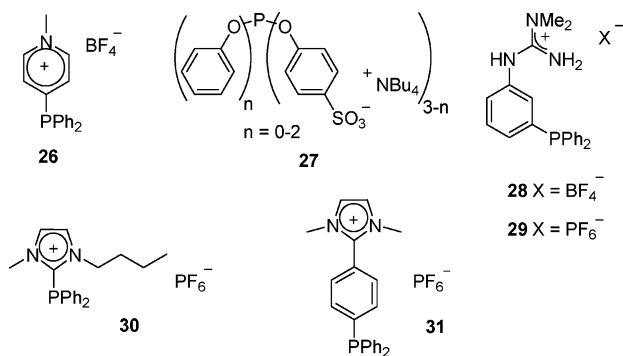
**Scheme 9. Preparation Route to Cobaltocenium-Based Phosphine Ligands<sup>66</sup>****Table 11. Rh-Catalyzed Hydroformylation<sup>a</sup> of 1-Octene in [BMIM][PF<sub>6</sub>] with Ligands **23** and **25**<sup>66</sup>**

entry	ligand	TOF (h <sup>-1</sup> )	n/iso ratio	n-nonanal (%)
122	<b>1</b>	426	2.6	72
123	<b>19</b>	98	2.6	72
124	dppe	35	3.0	75
125	dppf	828	3.8	79
126	<b>25</b>	66	2.6	73
127	<b>23</b>	810	16.2	94

<sup>a</sup> Reaction conditions:  $p(\text{H}_2/\text{CO} = 1:1) = 10$  bar,  $T = 100$  °C,  $t = 1$  h, Rh(acac)(CO)<sub>2</sub> precursor, ligands/Rh = 2, 1-octene/Rh = 1000, 5 mL of [BMIM][PF<sub>6</sub>].

Complex **23** was synthesized from diphenylphosphinocobaltocene **21** by an improved procedure described by Herberich and Greiss<sup>67</sup> using an anaerobic oxidation method, and complex **25** was synthesized according to a procedure described by Coville et al.<sup>68</sup> The latter contains an alkyl bridge between the cyclopentadienyl rings and the phosphorus atoms in order to allow a more flexible ligand and to reduce the electron withdrawing influence of the cobaltocenium fragment on the phosphorus. The two ligands were tested in the hydroformylation of 1-octene in [BMIM][PF<sub>6</sub>] and compared with TPP (**1**), bidentate ligands 1,2-bis(diphenylphosphino)ethane (dppe) and 1,1'-bis(diphenylphosphino)ferrocene (dppf), as well as the sulfonated TPPTS (**19**). Table 11 summarizes the results.

With TPP (**1**) as ligand, a high reaction rate was obtained, but the organic phase became deep yellow colored after the reaction, due to significant Rh leaching. TPPTS (**19**) as ligand gave much lower TOF but an improved catalyst retention in the ionic liquid. With the exception of **23**, all ligands tested gave the same selectivity toward n-nonanal, around 75%. Notably, ligand **23** showed exceptionally higher activity than the isoelectronic and isostructural ligand dppf. This was attributed to the electron withdrawing effect of the cobaltocenium fragment, which allowed improved back-bonding from the metal center. This effect was also claimed to be responsible for the lower activity and selectivity of ligand **25**, since the alkyl bridge lowers the electron withdrawing ability of the cobaltocenium. Rh leaching was less than 0.2% for both ionic ligands **23** and **25**, and recycling experiments showed unchanged activity and selectivity.

**Scheme 10. Structures of Phosphine and Phosphite Ligands Containing Ionic Tags**

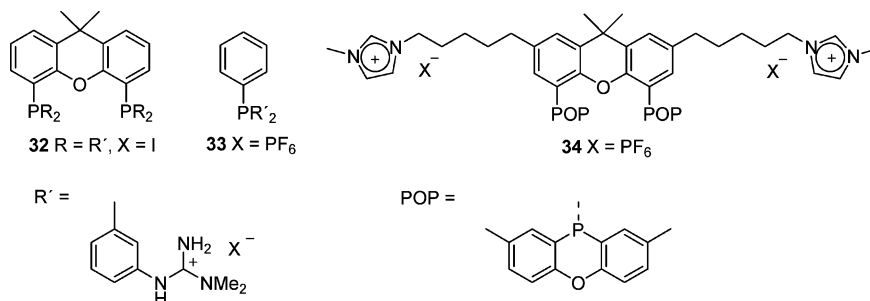
Alternatively, methods to immobilize phosphine ligands by attaching them to ionic groups with high similarity to the ionic liquid cations have been reported.<sup>57,69</sup> In Scheme 10, ligands **26–31** with ionic tags attached are shown.

Ligands **26–29** have been applied by Olivier-Bourbigou and co-workers in 1-hexene hydroformylation in [BMIM][BF<sub>4</sub>] and [BMIM][PF<sub>6</sub>].<sup>57</sup> The use of the monophosphine ligands **26**, **28**, and **29** resulted in moderate selectivity, between 72 and 80% *n*-heptanal, and TOF between 180 and 240 h<sup>-1</sup>. Minor rhodium leaching was observed when using the guanidinium-based ligand **29** in the ionic liquid [BMIM][BF<sub>4</sub>]. The monophosphite ligand **27** showed high selectivity of 93% *n*-heptanal with an initial TOF about 240 h<sup>-1</sup>. The activity decreased during two recycling experiments to 60 h<sup>-1</sup> while the selectivity remained constant.

Ligands **30** and **31** were tested in the biphasic hydroformylation of 1-octene in [BMIM][PF<sub>6</sub>].<sup>69</sup> In the case of ligand **30** a highly active system (TOF of 552 h<sup>-1</sup>) but less selective one (52% *n*-nonanal) was obtained, whereas in the case of ligand **31** the TOF was 51 h<sup>-1</sup> and the selectivity improved to 74%. The low selectivity is not surprising, since both ligands are quite similar to TPP (**1**).

For highly regioselective hydroformylation of 1-octene in [BMIM][PF<sub>6</sub>], Wasserscheid et al. synthesized phenylguanidinium modified xantphos ligands based on xanthene (**32**) and TPP (**33**) structures as depicted in Scheme 11.<sup>70</sup> Results from the recycling experiments are summarized in Table 12.

Again, TPP ligand **1** gave high initial rates but resulted in significant Rh leaching. After the first cycle, 53% of the Rh inventory was found in the organic phase (detected by ICP). Alternatively, TPPTS (**19**) allowed good immobilization of Rh but provided much lower rates. When using the monodentate phenylguanidinium ligand (**33**), the Rh leaching was below the detection limit (ICP < 0.07%), and the activity increased during the recycling experiments due to catalyst preformation. The bidentate phenylguanidinium ligand **32** showed excellent selectivity toward *n*-nonanal of about 95%

**Scheme 11. Structures of Phenylguanidinium and Phenoxaphosphino Modified Xantphos Ligands****Table 12. Rh-Catalyzed Hydroformylation<sup>a</sup> of 1-Octene in [BMIM][PF<sub>6</sub>] with Ligands **32** and **33**<sup>70</sup>**

entry	ligand	cycle	conversion (%)	TOF (h <sup>-1</sup> )	S <sub>hyd+iso</sub> (%)	<i>n</i> -nonanal (%)
128	<b>1</b>	1	69.1	680	0.4	73.7
129	<b>1</b>	3	10.2	100	0.1	73.0
130	<b>19</b>	1	7.8	80	4.9	72.2
131	<b>19</b>	2	7.7	78	4.9	72.2
132	<b>33</b>	1	32.1	276	2.5	66.6
133	<b>33</b>	3	35.3	330	3.5	63.0
134	<b>32</b>	1	10.6	15	1.5	95.0
135	<b>32</b>	3	21.9	30	2.4	95.4
136	<b>32</b>	5	38.3	52	3.4	95.5
137	<b>32</b>	7	44.3	58	3.9	94.7

<sup>a</sup> Reaction conditions: *p*(H<sub>2</sub>/CO = 1:1) = 30 bar, *T* = 100 °C, Rh(acac)(CO)<sub>2</sub> precursor (preformation time = 0.5 h), ligands/Rh = 2, 1-octene/Rh = 1000, 5 mL of [BMIM][PF<sub>6</sub>], *t* = 1 h (entries 128–132) and 8 h (entries 133–137).

**Table 13. Rh-Catalyzed Hydroformylation<sup>a</sup> of 1-Octene in [BMIM][PF<sub>6</sub>] with Ligand **34**<sup>71</sup>**

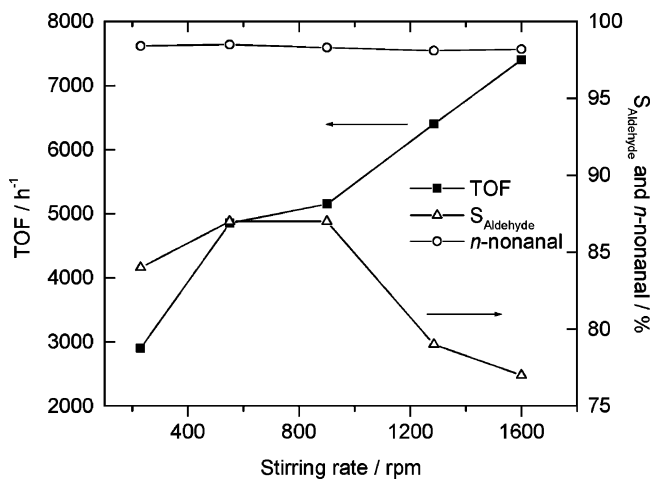
entry	ligand	cycle	TOF (h <sup>-1</sup> )	<i>n</i> -nonanal (%)	S <sub>ald</sub> (%)	S <sub>iso</sub> (%)
138	<b>34</b>	1	65	97.8	86.2	11.8
139	<b>34</b>	2	88	98.0	89.8	8.3
140	<b>34</b>	3	93	97.8	90.1	7.8
141	<b>34</b>	4	112	97.8	90.3	7.7
142	<b>34</b>	5	107	97.4	88.1	9.6
143	<b>34</b>	6	318	98.0	85.0	13.3
144	<b>34</b>	7	305	98.2	80.8	17.7

<sup>a</sup> Reaction conditions: *p*(H<sub>2</sub>/CO = 1:1) = 17 bar (entries 138–142) and *p*(H<sub>2</sub>/CO = 6.7:1) = 46 bar (entries 143–144), *T* = 100 °C, 5 mg of Rh(acac)(CO)<sub>2</sub> precursor, **34**/Rh = 4, 1-octene/Rh = 988, 3 mL of [BMIM][PF<sub>6</sub>], reactions stopped at about 30% conversion.

during all recycling experiments, with no Rh leaching detected. The activity increased also due to catalyst preformation and possibly gradual removal of impurities, though it remained low compared to that for the other examined ligands.

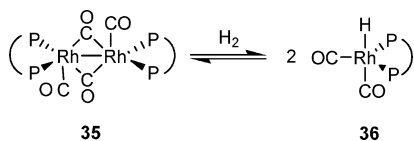
A dicationic phenoxaphosphino modified xantphos type ligand **34** (see Scheme 11) was reported by van Leeuwen et al. in 2002.<sup>71</sup> The ligand gave excellent results in the rhodium-catalyzed hydroformylation of 1-octene in [BMIM][PF<sub>6</sub>] with no Rh and P leaching being detected throughout seven recycling experiments. The results are summarized in Table 13.

Also here, a preformation period was observed during the first recycles (entries 138–141), after which the catalyst activity reached a constant TOF level around 110 h<sup>-1</sup>. This low activity was attributed to the presence of dimeric rhodium species which are inactive in the hydroformylation.<sup>72</sup> In order to shift the equilibrium toward the active monomeric rhodium-hydride species, the partial pressure of hydrogen



**Figure 9.** Effect on the stirring rate in Rh-**34**-catalyzed hydroformylation of 1-octene. Reproduced based on data from ref 73. (Reaction conditions:  $p(\text{H}_2/\text{CO} = 9:1) = 60$  bar,  $T = 100$  °C, Rh(acac)(CO)<sub>2</sub> precursor, [Rh] = 1.7 mM, [**34**] = 27 mM, 1-octene/Rh = 3823, 3 mL of [BMIM][PF<sub>6</sub>], TOF and selectivity determined after 40% conversion.)

**Scheme 12. Equilibrium between Dimeric Rhodium Carbonyl Complex and Monomeric Rhodium Hydride Complex<sup>72,73</sup>**



was increased in subsequent cycles. Indeed, higher TOF values were observed in the last two runs (entries 143 and 144). Besides the high selectivity and good activity in [BMIM][PF<sub>6</sub>], the catalytic system proved to be very stable and could be stored under air for more than 14 days without loss of activity.

An extended study on the dicationic phenoxaphosphino modified xantphos ligand **34** has additionally been reported by van Leeuwen et al.<sup>73</sup> Complementary to the earlier reported results, they investigated the effect of stirring speed and catalyst concentration on the hydroformylation of 1-octene. When decreasing the rhodium concentration from 6.4 to 1.7 mM, a dramatic increase in the activity together with a slight increase in regioselectivity was observed, as shown in Figure 9.

The variation of TOF with stirring speed indicated that the system was operating under mass transport limitations even at 1600 rpm. Moreover, increasing stirring speed resulted in higher isomerization tendency of the catalyst, attributed to different dissolution rates of the reactants. Reducing the ligand concentration from 27 to 7 mM had a positive effect on the activity while the selectivity toward *n*-nonanal remained unchanged. Furthermore, syngas pressure variations indicated that rhodium dimer species **35** were still present even at those very low rhodium concentrations but

**Table 14. Rh-Catalyzed Hydroformylation<sup>a</sup> of 1-Octene in [HMIM][PF<sub>6</sub>] with Ligand **34**<sup>73</sup>**

entry	ligand	cycle	TOF (h <sup>-1</sup> )	<i>n</i> -heptanal (%)	S <sub>ald</sub> (%)	S <sub>iso</sub> (%)
145	<b>34</b>	1	1400	97.6	87	10.8
146	<b>34</b>	2	4950	97.8	92	5.9
147	<b>34</b>	3–6	9000	97.8	81	16.6
148	<b>34</b>	7–9	5250	97.7	79	19.0

<sup>a</sup> Reaction conditions:  $p(\text{H}_2/\text{CO} = 9:1) = 60$  bar (entries 145–147) and  $p(\text{H}_2/\text{CO} = 1:1) = 12$  bar (entries 148),  $T = 100$  °C, Rh(acac)(CO)<sub>2</sub> precursor, [Rh] = 1.7 mM, [**34**] = 7 mM, 1-octene/Rh = 3823, 3 mL of [HMIM][PF<sub>6</sub>], stirring rate = 900 rpm, TOF and selectivity determined after 40% conversion.

that the equilibrium was shifted almost completely toward monomeric rhodium hydride species **36**, as shown in Scheme 12.

When using the catalyst system for the hydroformylation and isomerization of *trans*-2-butene, severe catalyst deterioration was observed at 120 °C and reduced CO partial pressure. Furthermore, both Rh and P leaching were detected and a low selectivity indicated the formation of unmodified rhodium species.

Hydroformylation of 1-hexene using the same system under optimized reaction conditions resulted in significant Rh leaching into the organic phase and possible catalyst decomposition, in strong contrast to the analogue 1-octene experiments, where no leaching was observed. However, when the ionic liquid was changed from [BMIM][PF<sub>6</sub>] to the homologue [HMIM][PF<sub>6</sub>], a stable catalyst system was obtained again with only minor Rh leaching detected by ICP (0.07–0.08%).<sup>73</sup> Table 14 summarizes these results.

In 2007 Peng et al. reported the use of amphiphilic phosphine ligands for biphasic hydroformylation in ionic liquid systems.<sup>74</sup> The bulky phosphines **37–39** contained different numbers of sulfonated groups, as depicted in Scheme 13.

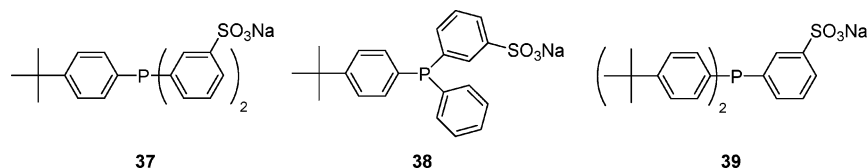
Ligand **37** was tested against the classical TPPTS ligand **19** in the hydroformylation of 1-hexene in the ionic liquid [BMIM][BF<sub>4</sub>]. The performance of both catalysts was comparable, with around 60% conversion and between 75 and 80% *n*-heptanal being formed. In Table 15, selected results from recycling experiments and ionic liquid variation are compiled. Not surprisingly, both Rh and ligand leaching into the organic phase (detected by ICP) were significantly higher in the case of the amphiphilic ligand **37** (compare entries 149–151 with entries 152–154).

Notably, in the more hydrophobic ionic liquid [BMIM][PF<sub>6</sub>], the activity of the TPPTS modified Rh catalyst was very low (entry 157), while the amphiphilic systems offered higher activities at similar selectivity.

**3.2.2. Chiral Ligands**

The first study on stereoselective biphasic hydroformylation in ionic liquids was reported by Deng et al. in 2007 using the asymmetric sulfonated ligand (*R*)-BINAPS (**42**) in the ionic liquid [BMIM][BF<sub>4</sub>] for the enantioselective

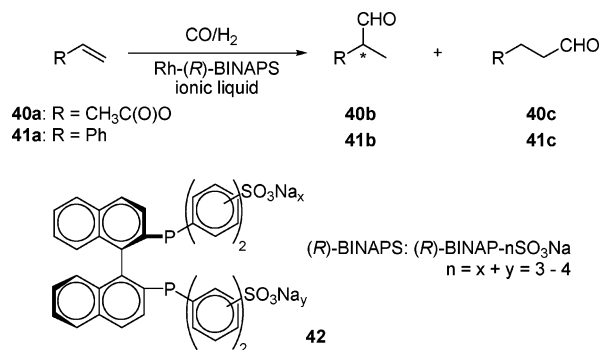
**Scheme 13. Structures of Amphiphilic (*m*-Sulfonatophenyl)arylphosphine Ligands**



**Table 15. Rh-Catalyzed Hydroformylation<sup>a</sup> of 1-Hexene Using Amphiphilic Phosphine Ligands<sup>74</sup>**

entry	solvent	ligand	cycle	conversion (%)	<i>n</i> -heptanal (%)	TOF (h <sup>-1</sup> )	Rh leaching (ppb)	P leaching (ppb)
149	[BMIM][BF <sub>4</sub> ]	<b>19</b>	1	44.9	78.3	92	10	49
150		<b>19</b>	2	62.2	76.2	124	10	66
151		<b>19</b>	3	61.5	72.2	123	4	32
152		<b>37</b>	1	64.5	79.6	129	66	337
153		<b>37</b>	2	65.0	77.8	130	50	216
154		<b>37</b>	3	66.5	75.0	133	23	105
155		<b>38</b>	1	84.4	77.3	169		
156		<b>39</b>	1	58.5	74.4	117		
157	[BMIM][PF <sub>6</sub> ]	<b>19</b>	1	3.7	73.0	7		
158		<b>37</b>	1	60.2	77.3	120		
159		<b>38</b>	1	87.3	79.2	174		
160		<b>39</b>	1	84.8	75.0	170		
161	[BMIM][ <i>n</i> -C <sub>12</sub> H <sub>25</sub> OSO <sub>3</sub> ]	<b>19</b>	1	86.6	77.8	173		
162		<b>37</b>	1	74.3	79.2	168		
163		<b>38</b>	1	83.7	75.6	148		
164		<b>39</b>	1	81.6	72.2	167		

<sup>a</sup> Reaction conditions: *p*(H<sub>2</sub>/CO = 1:1) = 15 bar, *T* = 100 °C, *t* = 4 h, L/Rh = 5, 1-hexene/Rh = 800, 2 mL of 1-hexene, 4 mL of ionic liquid, stirring rate = 800 rpm.

**Scheme 14. Asymmetric Hydroformylation of Vinyl Acetate and Styrene Using *m*-Sulfonated (*R*)-2,2'-(Diphenylphosphino)naphthalene ((*R*)-BINAPS) Ligands<sup>75</sup>**

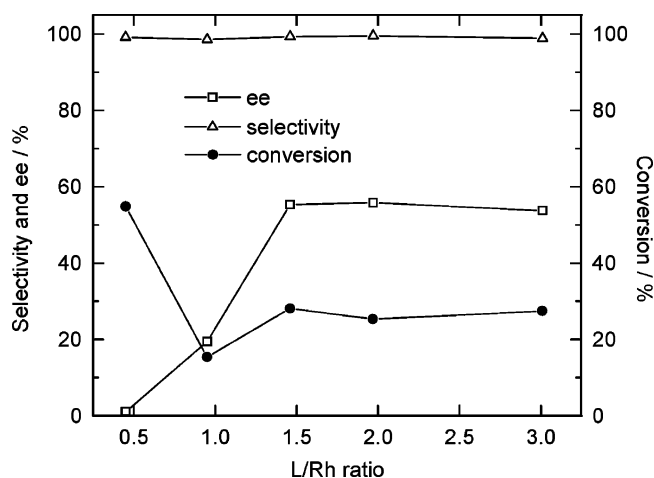
hydroformylation of vinyl acetate and styrene, as depicted in Scheme 14.<sup>75</sup>

Rh-(*R*)-BINAPS-catalyzed hydroformylation of vinyl acetate resulted in the predominant formation of 2-acetoxypropanal (**40b**) with an enantiomeric excess (ee) higher than 50%. The authors studied the effects of reaction conditions such as temperature, pressure, and ligand/rhodium ratio. Conversion and ee decreased slightly with increasing pressure, whereas the selectivity remained unchanged. At higher temperatures, higher conversion but lower ee were obtained. The maximum ee was obtained at L/Rh ratios higher than 1.5, as depicted in Figure 10.

The observed behavior led to the conclusion that the coordination chemistry in the biphasic ionic liquid toluene system was similar to the one observed in aqueous and homogeneous systems.<sup>76</sup> In a series of six consecutive recycling experiments, the Rh-(*R*)-BINAPS catalyst could be recovered without significant loss in activity or selectivity.

Styrene was hydroformylated under the same reaction conditions using the Rh-(*R*)-BINAP and Rh-(*R*)-BINAPS catalysts in two ionic liquids.<sup>75</sup> In the hydrophilic ionic liquid [BMIM][BF<sub>4</sub>], the (*R*)-BINAP modified catalyst showed 79% conversion with high selectivity for **41b** while the ee was moderate around 22%. The same catalyst only gave 64% conversion and an ee of only 6% in the hydrophobic [BMIM][PF<sub>6</sub>]. Using the sulfonated (*R*)-BINAPS ligand, the ee was low in both ionic liquids, as shown in Table 16.

Obviously, the nature of the ionic liquid had a significant influence on the catalytic performance in asymmetric hy-

**Figure 10.** Effect of L/Rh ratio on the asymmetric hydroformylation of vinyl acetate. Reproduced based on data from ref 75. (Reaction conditions: *p*(H<sub>2</sub>/CO = 1:1) = 10 bar, *T* = 60 °C, *t* = 24 h, 0.02 mmol Rh(acac)(CO)<sub>2</sub>, 1 mL of toluene, 2 mL of [BMIM][BF<sub>4</sub>], L = (*R*)-BINAPS (**42**), vinyl acetate/Rh = 300, stirring rate = 800 rpm.)**Table 16. Rh-Catalyzed Asymmetric Hydroformylation<sup>a</sup> of Styrene<sup>75</sup>**

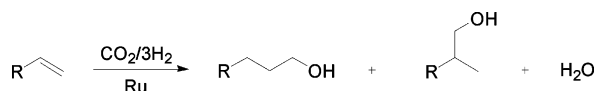
entry	ligand	solvent	ionic liquid	conversion (%)	ee (%)	<b>41b</b> (%)
165	( <i>R</i> )-BINAP	toluene	[BMIM][BF <sub>4</sub> ]	79.0	21.6	96.0
166	( <i>R</i> )-BINAP	toluene	[BMIM][PF <sub>6</sub> ]	64.1	6.0	94.0
167	( <i>R</i> )-BINAPS	toluene	[BMIM][BF <sub>4</sub> ]	56.3	8.1	94.2
168	( <i>R</i> )-BINAPS	toluene	[BMIM][PF <sub>6</sub> ]	61.6	8.0	89.5

<sup>a</sup> Reaction conditions: *p*(H<sub>2</sub>/CO = 1:1) = 20 bar, *T* = 60 °C, *t* = 24 h, 0.02 mmol of Rh(acac)(CO)<sub>2</sub>, 1 mL of toluene, 2 mL of ionic liquid, ligand/Rh = 1.5, styrene/Rh = 300, stirring rate = 800 rpm.

droformylation, the reason of which has not been clarified yet.

### 3.3. Carbon Dioxide as an Alternative Source of CO

A possible way to facilitate more benign hydroformylation reactions is to use nontoxic, abundant, and inexpensive carbon dioxide as reactant in place of carbon monoxide. In CO<sub>2</sub>-based hydroformylation, the reaction proceeds in two

**Scheme 15. Ru-Catalyzed Alkene Hydroformylation with CO<sub>2</sub> via the Reverse Water-gas Shift (RWGS) Reaction**


consecutive steps, where CO<sub>2</sub> and hydrogen initially are converted into CO and water via the reverse water-gas shift (RWGS) reaction, whereafter the generated CO becomes the reagent of hydroformylation of the substrate.<sup>77,78</sup> Normally, however, the major reaction product is not the aldehyde but the corresponding alcohol due to facile reduction of the aldehyde produced in the presence of hydrogen, according to Scheme 15. Furthermore, the presence of halide ions has proven essential for CO<sub>2</sub> activation with Ru complexes in the RWGS reaction, and increased catalyst activity in the order of I<sup>-</sup> < Br<sup>-</sup> < Cl<sup>-</sup>, corresponding to the order of halide proton affinity, has been reported.<sup>79,80</sup>

The first Ru-catalyzed CO<sub>2</sub>-based hydroformylation in ionic liquid was reported by Tominaga and Sasaki.<sup>81,82</sup> They applied Ru<sub>3</sub>(CO)<sub>12</sub> clusters dissolved in organic/ionic liquid systems to hydroformylate 1-hexene directly to heptanols (via additional reduction) in batch mode. The results were further compared to an analogous reaction in *N*-methyl-2-pyrrolidone (NMP), which is known to be an effective solvent for reaction of terminal alkenes, though it only provides modest chemoselectivity toward hydroformylation products due to competing alkene hydrogenation. With a toluene/[BMIM]-Cl system, the reaction gave an almost equimolar mixture of C<sub>7</sub> alcohols in 84% yield along with 11% hexane but no aldehydes, while the yields of the alcohols, hexane, and aldehydes remained 64%, 25%, and 5%, respectively, with NMP. Moreover, the reaction mixture spontaneously phase separated into organic and ionic liquid layers (in contrast to reaction in NMP), allowing the ionic liquid catalyst phase to be reused for two additional runs before the catalytic activity decreased due to accumulation of water suppressing the CO formation in the RWGS reaction. Ionic liquids with anions other than chloride were found to be much less effective, most probably due to their instability toward hydrolysis by the water formed in the RWGS reaction. Thus, even in the presence of a small amount of a chloride salt, the hydroformylation in [BMIM][BF<sub>4</sub>] gave lower yield and chemoselectivity toward alcohols (63% alcohols), while [BMIM][PF<sub>6</sub>] induced catalyst degradation, probably caused by the hydrolysis products, and only very low formation of hydroformylation products (86% alkane). Additionally, [BMPyr]Cl was found to give a considerable amount of hydroformylation products (65% alcohols, 10% alkane) but degraded as the alcohols were produced.

In recent work, Tominaga reported an improved version of the CO<sub>2</sub>-based Ru<sub>3</sub>(CO)<sub>12</sub>/ionic liquid 1-hexene hydroformylation reaction where use of volatile organic cosolvent proved unnecessary.<sup>83</sup> Here, replacement of up to half the chloride anions in [BMIM]Cl with [Tf<sub>2</sub>N]<sup>-</sup> ions resulted in increased heptanol yields up to 82% (TOF around 16 h<sup>-1</sup>), as a result of gradually increased solubility of 1-hexene in the ionic liquid phase. However, at mole fractions above 0.5, where the alcohol yield reached a maximum, the yield decreased due to aldol condensation of intermediately formed heptanal and due to the [Tf<sub>2</sub>N]<sup>-</sup> anion being ineffective in the activation of CO<sub>2</sub>. Replacement of chloride ions with [BF<sub>4</sub>]<sup>-</sup> anions was also found to be effective, but the alcohol yield was slightly decreased. In contrast, replacement with [PF<sub>6</sub>]<sup>-</sup> anions caused catalyst degradation (possibly as a

**Table 17. Rh-Catalyzed Hydroformylation<sup>a</sup> of 1-Hexene with CO<sub>2</sub> as the Carbon Monoxide Source<sup>83</sup>**

entry	reaction media	conversion (%)	yield (%)		
			heptanol	heptanal	hexane
169	[BMIM]Cl	75.4	50.3	2.3	3.9
170	[BMIM][Cl/Tf <sub>2</sub> N]	94.0	82.0	0	8.5
171	[BMIM][Cl/BF <sub>4</sub> ]	95.2	71.0	0	9.1
172	[BMIM][Cl/PF <sub>6</sub> ]	93.5	49.5	0	6.5
173	toluene/[BMIM]Cl	70.5	57.5	1.5	7.5
174	NMP	99.5	17.5	0.5	48.0

<sup>a</sup> Reaction conditions: *p*(H<sub>2</sub>/CO<sub>2</sub>) = 1:1 = 80 bar, *T* = 160 °C, *t* = 10 h, 0.1 mmol of Ru<sub>3</sub>(CO)<sub>12</sub>, 9.4 mmol of ionic liquid, X<sub>Cl</sub> = 0.5 (entries 170–172), 1-hexene/Ru = 200, 5 mL of organic solvent (entries 173 and 174).

**Table 18. Comparison of IR ν(CO) Bands of HRh(CO)<sub>2</sub>(ligand) Complexes in Different Solvent Systems**

entry	complex <sup>a</sup>	solvent	isomer	ν <sub>CO</sub> (cm <sup>-1</sup> )		ref
175	HRh(CO) <sub>2</sub> (7)	[BMIM][PF <sub>6</sub> ]	<i>ee</i>	2032	1967	88
			<i>ea</i>	1985	1935	
176	HRh(CO) <sub>2</sub> (6)	benzene	<i>ee</i>	2036	1969	89, 90
			<i>ea</i>	1991	1941	
177	HRh(CO) <sub>2</sub> (43)	cyclohexene	<i>ee</i>	2040	1977	89, 90
			<i>ea</i>	1999	1953	

<sup>a</sup> Ligand 6, xantphos; ligand 7, sulfoxantphos; ligand 43, thixantphos.

consequence of the hydrolytic degradation of [PF<sub>6</sub>]<sup>-</sup>) and much lower activity toward hydroformylation, as also previously reported with the biphasic organic/ionic liquid systems. In Table 17 the comparative results are compiled.

The influence of reaction temperature was also examined using the mixed [BMIM][Cl/Tf<sub>2</sub>N] ionic liquid. Here, the optimum hydroformylation temperature was found to be around 160 °C, whereas lower temperatures decreased the yield of heptanols and higher temperatures favored the direct hydrogenation of 1-hexene. Finally, recycling experiments confirmed only a slight decrease in catalytic activity after five consecutive runs, leading to a total decrease in heptanol yield of only 8%.

## 4. Spectroscopic and Mechanistic Studies of Hydroformylation Catalysts in Ionic Liquids

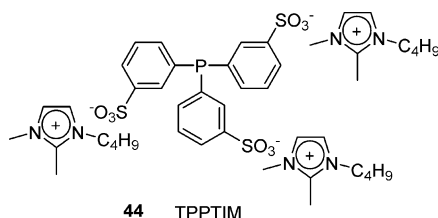
### 4.1. Rhodium Complex Catalysts

The great potential of in situ spectroscopic studies of catalysts in homogeneous hydroformylation has been explored in various publications.<sup>84–87</sup> In the last 5 years, powerful in situ spectroscopic techniques have been applied for studies in ionic liquid hydroformylation as well.

In the first work by van Leeuwen and Dupont et al. the Rh-sulfoxantphos (Rh-7)-catalyzed hydroformylation of 1-octene in [BMIM][PF<sub>6</sub>] ionic liquid has been followed by high pressure (HP) NMR and IR.<sup>88</sup> The red-brown solution of the rhodium dimer was observed to turn light yellow upon exposure to syngas at 40 °C. Bands at 2032, 1985, 1967, and 1935 cm<sup>-1</sup> in the IR spectrum were assigned to the two isomeric forms of the HRh(CO)<sub>2</sub>(7) complex. Furthermore, all bands were in good agreement with known absorptions for homogeneous rhodium complexes, as shown in Table 18.

Since the *ee*–*ea* equilibrium is influencing the *n/iso*-aldehyde selectivity of the diphosphine modified rhodium

**Scheme 16. Structure of 1-Butyl-2,3-dimethylimidazolium Tris(*m*-sulfonatotriphenyl)phosphine Ligand<sup>92</sup>**



catalysts, the equilibrium was studied at different temperatures and syngas pressures. With increasing temperature, the formation of the *ee*-complex was favored until a constant value was reached at 100 °C. The result was found to be in line with experimental findings where the *n/iso* selectivity increased with increasing temperature. With increasing syngas pressure, the equilibrium was shifted toward the *ea*-complex and should therefore give lower *n/iso* selectivity. This result was indeed observed for 1-octene hydroformylation.

The authors also investigated the formation of the rhodium hydride  $\text{HRh}(\text{CO})_2$  (**7**) in  $[\text{BMIM}][\text{PF}_6]$  via HP <sup>31</sup>P NMR ( $d^6$ -DMSO).<sup>88</sup> Under 10 bar syngas pressure, a sharp doublet at  $\delta (^1J_{\text{RhP}}) = 22.2$  (121 Hz) ppm indicated that the ligand mainly coordinated in an *ee*-fashion.<sup>91</sup> Signals in the range  $\delta = 0$ –10 ppm further indicated formation of the dimeric complex  $[\text{Rh}(\text{CO})(\mu\text{-CO})(\mathbf{7})]_2$ , which is formed in the presence of excess CO. This observation was explained by the CO solubility in  $[\text{BMIM}][\text{PF}_6]$ , which is much higher than the hydrogen solubility (see section 2.1). Additionally, in the hydroformylation of 1-octene, a slight increase in rate was observed with increasing hydrogen partial pressure.

In a second HP NMR study, the formation of phosphine modified rhodium species in  $[\text{BMIM}][\text{BF}_4]$  and  $[\text{BMIM}][\text{PF}_6]$  was studied by Mehnert and co-workers.<sup>92</sup> The monodentate phosphines TPP (**1**), TPPTS (**19**), and TPPTIM (**44**) (Scheme 16) were used at L/Rh ratios of 5 in this study. Ligand **44** was obtained from TPPTS via ion exchange using  $[\text{BMMIM}]\text{Cl}$  in acetonitrile.

NMR isotopic labeling studies with <sup>13</sup>C of the Rh–TPP system in toluene suggested in earlier studies the formation of two coordinatively unsaturated catalyst intermediates  $\text{HRh}(\text{CO})(\text{TPP})_2$  (**45a**) and  $\text{HRh}(\text{CO})_2(\text{TPP})$  (**46a**) from the saturated precomplexes  $\text{HRh}(\text{CO})(\text{TPP})_3$  (**47a**) and  $\text{HRh}(\text{CO})_2(\text{TPP})_2$  (**48a**), with the actual amount of the unsaturated species formed being strongly dependent on the syngas pressure. Both intermediates **45a** and **46a** are believed to be responsible for the production of aldehyde in the hydroformylation, while the *n/iso* ratio of the aldehydes produced is largely controlled by the competitive reactions of the alkene with the species, resulting in high or low *n/iso* ratios for **45a** and **46a**, respectively. Moreover, complex **47a** was found to be readily converted into complex **48a** already at a ( $\text{H}_2/\text{CO} = 1:1$ ) pressure of less than 20 bar. In contrast, investigation of  $\text{HRh}(\text{CO})(\text{TPPTS})_3$  (**47b**) in aqueous solution has revealed that not even pressures as high as 130 bar resulted in formation of the analogous complex  $\text{HRh}(\text{CO})_2(\text{TPPTS})_2$  (**48b**),<sup>93</sup> thus accounting partly for the abnormally high *n/iso* ratios observed in aqueous biphasic Rh–TPPTS-catalyzed hydroformylation.<sup>94</sup>

Initial experiments at 100 °C and 41 bar with the three different ligands in 1-hexene hydroformylation indicated that both the TPP (**1**) and the TPPTS (**19**) modified rhodium leached significantly from the  $[\text{BMIM}][\text{PF}_6]$  phase into the

organic 1-hexene phase.<sup>92</sup> TPPTIM (**44**) modified rhodium complexes only showed minor metal loss into the organic phase. It was found that TPPTS only had negligible solubility in  $[\text{BMIM}][\text{PF}_6]$  and—surprisingly—also in  $[\text{BMIM}][\text{BF}_4]$ . Despite the low solubility, the authors studied the formation of TPP and TPPTS modified rhodium complexes in  $[\text{BMIM}][\text{BF}_4]$  in the presence of syngas ( $\text{H}_2/\text{CO} = 1:1$ ). Hydride formation was observed already at 1 bar, as depicted in Figure 11.

In the obtained NMR spectra, signals from coordinated TPPTS ligand ( $\delta (^{31}\text{P}) = 32.2$  ppm, d), uncoordinated TPPTS oxide ( $\delta (^{31}\text{P}) = 29.1$  ppm, s), free ligand ( $\delta (^{31}\text{P}) = -3.7$  ppm, s), and coordinated <sup>13</sup>CO ( $\delta (^{13}\text{C}) = 195.2$  ppm, d) were all assigned. By comparison of the signals obtained in ionic liquid with those in  $d^8$ -toluene and water, the assumption was made that the structure of  $\text{HRh}(\text{CO})(\text{TPPTS})_3$  (**47b**) in  $[\text{BMIM}][\text{BF}_4]$  is similar to the known one of  $\text{HRh}(\text{CO})(\text{TPP})_3$  (**47a**) in  $d^8$ -toluene. Table 19 compiles selected results from the <sup>31</sup>P and <sup>13</sup>C NMR measurements.

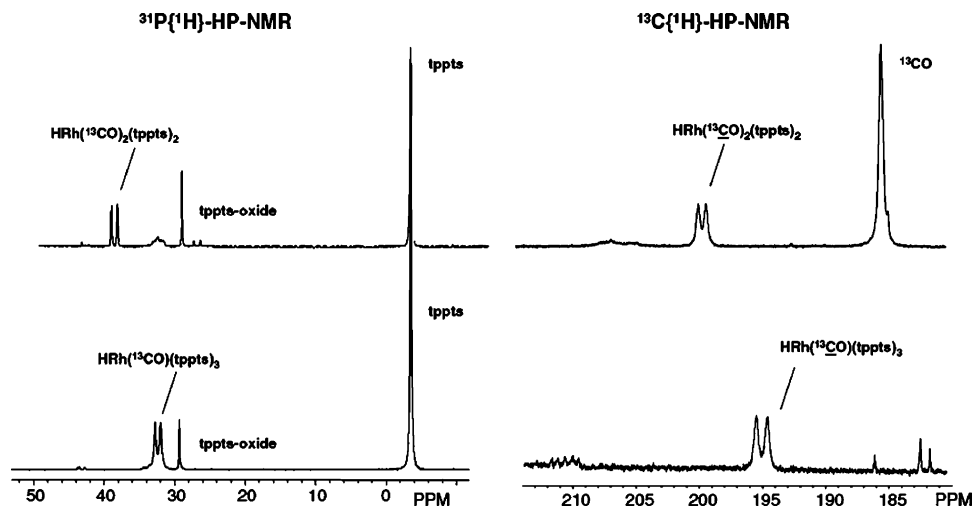
Upon stepwise increase of the pressure from 1 to 138 bar in the ionic liquid, a steady decrease in intensity of the <sup>31</sup>P signal originating from  $\text{HRh}(\text{CO})(\text{TPPTS})_3$  (**47b**) ( $\delta (^{31}\text{P}) = 32.2$  ppm, d) was observed, while signals ( $\delta (^{31}\text{P}) = 39.1$  ppm, d;  $\delta (^{13}\text{C}) = 199.2$  ppm, d) attributed to formation of complex  $\text{HRh}(\text{CO})_2(\text{TPPTS})_2$  (**48b**) (entry 179) appeared. After pressure release, the hydride  $\text{HRh}(\text{CO})(\text{TPPTS})_3$  (**47b**) was reformed.

In the same work, the catalytic activity of Rh-**44** in the biphasic hydroformylation of 1-hexene in  $[\text{BMIM}][\text{BF}_4]$  was investigated.<sup>92</sup> Batch recycling experiments at 100 °C and 41 bar indicated a rhodium loss of almost 10 wt % over 10 consecutive cycles. The linearity toward *n*-heptanal remained between 68 and 72%. When using the ionic liquid  $[\text{BMIM}][\text{PF}_6]$ , the rhodium loss increased significantly with only 85% of the initial rhodium being present in the reactor after the tenth cycle. Better retention of the rhodium in the ionic liquid phase was achieved upon increasing the L/Rh ratio from 10 to 100; however, this was accompanied by a lower activity. Compared with the homogeneous toluene system, all ionic liquid biphasic systems exhibited significantly lower activity due to mass transport limitations from the gas into the ionic liquid phase.

In order to evaluate the influence of mass transfer in ionic liquid biphasic systems, Sieffert and Wipff very recently<sup>95</sup> reported a molecular dynamics (MD) study of the interface involved in the biphasic 1-hexene hydroformylation system with Rh–PPh<sub>3</sub> and Rh–TPPTS catalysts in  $[\text{BMIM}][\text{PF}_6]$ . In the MD simulations (performed at 77 °C), a classical force field representation was applied, assuming all interactions to be mainly steric and electrostatic in nature, with the biphasic systems constituting two adjacent cubic boxes of bulk solvents (ca. 46 Å in length) and 255 ionic liquid ion pairs and 434 1-hexene or 355 1-heptanal molecules, respectively.

Initial simulations showed that no ionic liquid dissolved in the bulk (i.e., beyond 12 Å from the interface) of either of the organic phases, and only a few organic molecules diffused in the bulk ionic liquid phase on average during the dynamics. Moreover, no changes in the nature of the  $[\text{BMIM}][\text{PF}_6]/1$ -hexene interface were obtained in the presence of CO and H<sub>2</sub>, which mainly dissolved in the organic phase. However, on average, about twice as many CO as H<sub>2</sub> molecules were found to dissolve in the ionic liquid because CO diffused slowly due to entrapment in ionic liquid





**Figure 11.** High-pressure  $^{31}\text{P}\{^1\text{H}\}$  spectra (left) and  $^{13}\text{C}\{^1\text{H}\}$  spectra (right) of Rh-19 hydroformylation catalyst formed in the ionic liquid [BMIM][BF<sub>4</sub>] under syngas ( $\text{H}_2/^{13}\text{CO} = 1:1$ ) pressure of 138 bar (top) and 1 bar (bottom). Reproduced with permission from ref 92. Copyright 2004 Elsevier.

**Table 19.** NMR Data for Rh-phosphine Complexes Formed under Syngas in Different Solvent Systems<sup>92</sup>

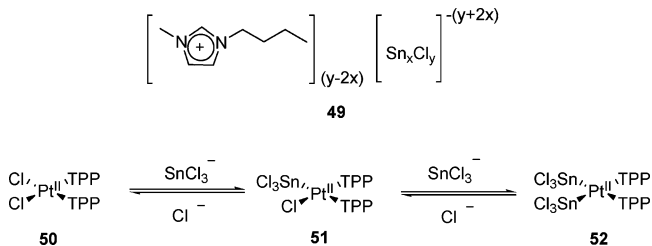
entry	solvent	pressure <sup>a</sup> (bar)	complex	$\delta$ ( $^{13}\text{CO}$ ) (ppm)	$^1J_{\text{Rh-C}}$ (Hz)	$\delta$ ( $^{31}\text{PR}_3$ ) (ppm)	$^1J_{\text{Rh-P}}$ (Hz)
178	[BMIM][BF <sub>4</sub> ]	1	$\text{HRh}(^{13}\text{CO})(\text{TPPTS})_3$	195.2	62	32.2	126
179	[BMIM][BF <sub>4</sub> ]	138	$\text{HRh}(^{13}\text{CO})_2(\text{TPPTS})_2$	199.2	61	39.1	137
180	<i>d</i> <sup>8</sup> -toluene	1	$\text{HRh}(^{13}\text{CO})(\text{TPP})_3$	206.6	62	37.8	156
181	<i>d</i> <sup>8</sup> -toluene	69	$\text{HRh}(^{13}\text{CO})_2(\text{TPP})_2$	199.9	63	33.8	139
182	H <sub>2</sub> O	1/207	$\text{HRh}(^{13}\text{CO})(\text{TPPTS})_3$	204.9	55	42.8	156

<sup>a</sup> Syngas: ( $\text{H}_2/^{13}\text{CO} = 1:1$ )

cavities, whereas H<sub>2</sub> rapidly exchanged between the ionic liquid and the 1-hexene phases. These results surmised that using overall higher H<sub>2</sub>/CO proportions should improve the hydroformylation reaction rate, since the reaction formally proceeds with stoichiometric amounts of CO and H<sub>2</sub> gas.

Additional “mixing–demixing” simulations involving Rh complexes in [BMIM][PF<sub>6</sub>]/1-hexene solution revealed further that neutral  $\text{HRh}(\text{CO})(\text{TPP})_3$  complexes had a clear preference for the 1-hexene phase of the interface whereas  $\text{HRh}(\text{CO})(\text{TPPTS})_3$  containing charged ligands preferred the ionic liquid side due to strong solvation of the ligand sulfonate groups with [BMIM]<sup>+</sup> cations. Interestingly, both rhodium precatalysts were, however, found to be located relatively close to the interface instead of being situated near the center of the liquid slabs where they are more soluble. In the case of neutral  $\text{HRh}(\text{CO})(\text{TPP})_3$  complexes, they, although mostly surrounded by 1-hexene molecules, displayed loose contacts with the ionic liquid at the interface and with the butyl chain of the [BMIM]<sup>+</sup> ions immersed in the 1-hexene phase, making them quite mobile and facilitating their exchange from one interface to the other. On the contrary, the  $\text{HRh}(\text{CO})(\text{TPPTS})_3$  precatalyst remained firmly immobilized in the ionic liquid with a solvation shell of [BMIM]<sup>+</sup> cation in contact with the organic phase, preventing bulk and interfacial exchange. Nonetheless, less charged and more amphiphilic reaction intermediates such as, e.g.,  $\text{HRh}(\text{CO})_2(\text{TPPTS})_2$  and  $\text{HRh}(\text{CO})(\text{TPPTS})_2(1\text{-hexene})$  complexes with formal ligand charges of  $-6$ , and dissolved TPPTS ligands with formal charges of  $-3$ , being more surface active than the precatalyst itself, could facilitate reaction by bringing the metal center closer to the reaction interphase.

**Scheme 17.** Pt–TPP-Catalyzed Hydroformylation in 1-Butyl-3-methylimidazolium Chlorostannates<sup>96</sup>

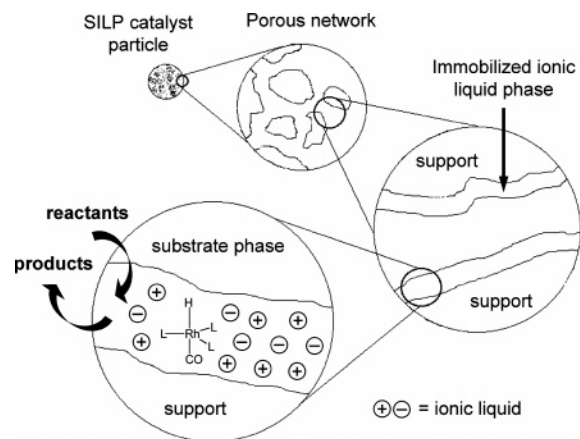


## 4.2. Platinum Complex Catalysts

The mechanism of Pt-catalyzed hydroformylation in both chlorostannate melts **49** (Scheme 17) and [BMIM][Tf<sub>2</sub>N] has been studied by van Eldik and co-workers.<sup>96</sup>

The active species were formed from *cis*-Pt(TPP)<sub>2</sub>Cl<sub>2</sub> (**50**) upon addition of cocatalyst SnCl<sub>2</sub> (Scheme 17) and were studied using UV–vis and NMR spectroscopy. No reaction was observed below a molar ratio of 0.5 of *cis*-Pt(TPP)<sub>2</sub>Cl<sub>2</sub> to SnCl<sub>2</sub>. At a ratio of 0.5, only a slow, single-step reaction occurred, while the reaction changed into a two-step process at SnCl<sub>2</sub> molar ratios above 0.5.

In a second series of experiments, the chlorostannate melts were dissolved in the ionic liquid [BMIM][Tf<sub>2</sub>N]. Kinetic measurements at room temperature at several SnCl<sub>3</sub><sup>-</sup> concentrations indicated a two-step process similar to the one observed in pure chlorostannate melts. The fast, first reaction step showed first order behavior, and the observed rate constant was linearly dependent on the SnCl<sub>3</sub><sup>-</sup> concentration, suggesting the reaction to be the nucleophilic substitution of chloride by SnCl<sub>3</sub><sup>-</sup> to yield *cis*-Pt(TPP)<sub>2</sub>Cl(SnCl<sub>3</sub>) (**51**). The second, relatively slow reaction step could not be verified due to precipitation of side products. Additionally, the authors



**Figure 12.** Schematic drawing of a supported ionic liquid-phase (SILP) catalyst.

performed hybrid DFT calculations (B3LYP/LANL2DZp level) using GAUSSIAN in order to test different pathways for the formation of  $\text{Pt}(\text{PH}_3)_2\text{Cl}(\text{SnCl}_3)$ , where  $\text{PH}_3$  was used for simplification purposes instead of TPP. The modeling supported the experimental findings that the formation of  $\text{Pt}(\text{TPP})_2\text{Cl}(\text{SnCl}_3)$  (**51**) should proceed via insertion of  $\text{SnCl}_2$  in a Pt–Cl bond in chlorostannate melts, whereas in  $[\text{BMIM}][\text{Tf}_2\text{N}]$  the substitution of chloride by  $\text{SnCl}_3^-$  should be the governing step.

## 5. Hydroformylation with Ionic Liquids in Alternative Reaction Systems

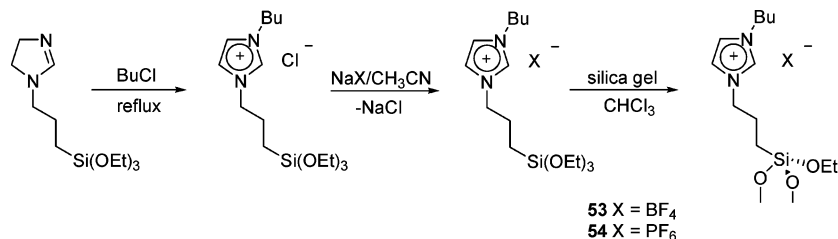
### 5.1. Supported Ionic Liquid-Phase (SILP) Systems

When a substantial amount of an ionic liquid is immobilized on a porous solid support material, the formation of multiple layers of free ionic liquid on the carrier may act as an inert reaction phase to dissolve various homogeneous catalysts. Although such supported ionic liquid-phase (SILP) catalysts appear as solids, the active species dissolved in the ionic liquid phase on the support maintain the attractive features of ionic liquid homogeneous catalysts such as, e.g., high specificity and dispersion of molecular entities. In Figure 12, a SILP hydroformylation catalyst is schematically shown.

#### 5.1.1. Batch Mode Reactions

The first example using SILP catalysts for hydroformylation was reported by Mehnert and co-workers in 2002.<sup>97</sup> Here, Rh-SILP catalysts based on silica gel support modified with a monolayer of covalently anchored ionic liquid fragments of 3-triethoxysilylpropylimidazolium (average of 0.4 ionic liquid fragments per  $\text{nm}^2$ ) were prepared according to Scheme 18. Impregnation of the modified silica **53** or **54** with additional ionic liquid,  $\text{Rh}(\text{acac})(\text{CO})_2$ , and the ligand TPPTS (**19**) or TPPTIM (**44**) (structure in Scheme 16)

**Scheme 18.** Preparation Route of Silica SILP Material Modified with 3-Triethoxysilylpropylimidazolium Fragments<sup>97</sup>



**Table 20.** Rh-Catalyzed Hydroformylation<sup>a</sup> of 1-Hexene Using SILP, Biphasic, and Homogeneous Catalysis<sup>97</sup>

entry	condition	ligand	solvent	time (h)	yield (%)	<i>n</i> -heptanal (%)	TOF ( $\text{h}^{-1}$ )
183	SILP	<b>44</b>	$[\text{BMIM}][\text{BF}_4]$	5	33	70.6	3900
184	SILP	<b>19</b>	$[\text{BMIM}][\text{BF}_4]$	4	40	70.6	3360
185	SILP	<b>44</b>	$[\text{BMIM}][\text{PF}_6]$	4.5	46	70.6	3600
186	SILP	none	$[\text{BMIM}][\text{PF}_6]$	3	85	28.6	11400
187	biphasic	<b>44</b>	$[\text{BMIM}][\text{BF}_4]$	3.2	58	68.8	1380
188	biphasic	<b>44</b>	$[\text{BMIM}][\text{PF}_6]$	3	70	71.4	1320
189	biphasic	<b>19</b>	$\text{H}_2\text{O}$	6	11	95.8	144
190	homogen	<b>1</b>	toluene	2	95	72.2	24000

<sup>a</sup> Reaction conditions:  $p(\text{H}_2/\text{CO}_2 = 1:1) = 100$  bar (entries 183–186) and 40 bar (entries 187–190),  $T = 100$  °C,  $\text{Rh}(\text{acac})(\text{CO})_2$  precursor, ligands/Rh = 10, TOF determined at full conversion.

resulted in a multiple ionic liquid catalyst layer corresponding to an ionic liquid-phase loading of 25 wt %.

The SILP catalysts were applied for hydroformylation of 1-hexene using both homogeneous and liquid–liquid biphasic process design under harsh conditions. The obtained results are compiled in Table 20.

The hydroformylation activities of the obtained Rh-SILP catalysts were found to be almost three times higher than those for comparable biphasic systems (TOF of 3360–3600  $\text{h}^{-1}$  versus 1320–1380  $\text{h}^{-1}$ ), which was attributed to a higher rhodium concentration at the large reaction interface. Also, a comparable low selectivity around 71% *n*-heptanal was obtained, as expected for monophosphine catalysts. Notably, at higher conversions, rhodium leaching (up to 2.1 mol %) accompanied by significant depletion of the supported ionic liquid layer occurred, as a result of gradually increased ionic liquid solubility in the reaction mixture and—possibly unavoidable—entrainment of the liquid film induced by intensive stirring. The metal loss could, however, be somewhat suppressed at lower aldehyde concentrations and higher ligand excess in single runs. Nonetheless, pronounced catalyst deactivation was apparently found, even at lower conversion, during recycling of the catalyst, independently of the presilylation of the support. For further comparison, the aqueous biphasic reaction and the conventional homogeneous catalyst in toluene were investigated under similar reaction conditions. As expected, the aqueous system was significantly less active due to low substrate solubility in the aqueous phase but gave high *n*-heptanal selectivity around 96%. The homogeneous catalyst system, however, exhibited a very high TOF of 24000  $\text{h}^{-1}$  but did not benefit from the attractive advantage of convenient product separation as the supported catalysts.

SILP Rh-TPPTS catalysts have also been prepared by immobilizing the complexes in the ionic liquids  $[\text{BMIM}][\text{PF}_6]$ ,  $[\text{BMIM}][\text{BF}_4]$ , and 1,1,3,3-tetramethylguanidinium lactate (TMGL) supported on mesoporous MCM-41.<sup>98</sup> For 1-hexene hydroformylation, catalyst activity was found to be strongly dependent on the degree of ionic liquid pore

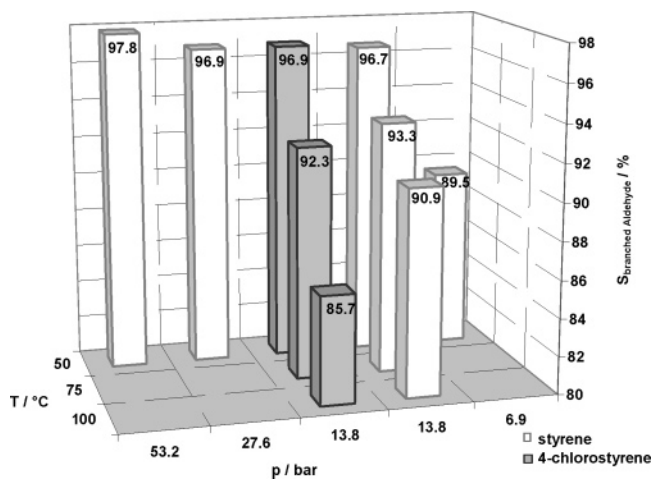
filling, i.e., ionic liquid loading (ratio between ionic liquid volume and pore volume of support), and also on the silica support, with the highest TOF (up to 389 h<sup>-1</sup>) obtained at ionic liquid loadings between 0.08 and 0.13 (corresponding to 10–15 wt %) for MCM-41 catalysts. The obtained selectivity of up to 77.8% for *n*-heptanal was slightly higher compared to previously published results for monodentate Rh catalysts. Moreover, recycling experiments with Rh-TPPTS dissolved in TMGL on MCM-41 support demonstrated, in contrast to the other ionic liquids, no deactivation after 11 cycles, clearly indicating the metal complex to be retained within the ionic liquid film. The authors explained this behavior by a slightly coordinating ability of TMGL to the rhodium atom.

The same authors reported on the structural characterization of the Rh-TPPTS SILP systems.<sup>99</sup> X-ray powder diffraction (XRD) studies on MCM-41 with various ionic liquid loadings indicated that no structural changes to the support were facilitated by the ionic liquid film, while scanning electron microscopy (SEM) images established a smoothed morphology for the ionic liquid loaded support. Moreover, nitrogen absorption/desorption isotherms on catalysts revealed decreasing specific surface area, pore volume, and mean pore diameter with increasing ionic liquid loading. The shape of the isotherms indicated, however, no significant differences in ionic liquid dispersion in the mesopores of the support before and after heating at conditions resembling reaction. This was further supported by high-resolution transmission electron microscopy (HRTEM) images, eventually leading to the conclusion that the ionic liquid film remained stable on the MCM-41 support.

The catalytic species present in the SILP catalyst was further studied by means of FT-IR and NMR spectroscopy. FT-IR data of fresh SILP systems indicated the catalytic precursor Rh(acac)(CO)<sub>2</sub> ( $\nu_{\text{CO}} = 2080, 2010 \text{ cm}^{-1}$ ) and the resting state of the active species HRh(CO)(TPPTS)<sub>3</sub> (**47b**) ( $\nu_{\text{CO}} = 1984 \text{ cm}^{-1}$ ), with the latter exclusively observed for used SILP systems. Furthermore, <sup>31</sup>P NMR data revealed the presence of active Rh-TPPTS species ( $\delta (^1J_{\text{Rh-P}}) = 32 \text{ ppm}$  (130 Hz), d) clearly indicating the homogeneous nature of the SILP Rh-TPPTS complex catalyst systems contained as a highly dispersed phase on the internal surface of the porous support.

Recently, ionic liquid immobilization within a silica sol-gel matrix has been reported for the rhodium-catalyzed hydroformylation of vinylarenes to branched aldehydes.<sup>100</sup> The catalyst was formed by mixing the precursor [Rh(COD)-Cl]<sub>2</sub>, ligand TPPMS (**2**), prehydrolyzed Si(OCH<sub>3</sub>)<sub>4</sub>, and modified ionic liquid 1-butyl-3-[3-(trimethoxysilyl)propyl]imidazolium chloride in THF for 6 h. Aging at room temperature for 12 h and removal of the solvent resulted in the sol-gel entrapped ionic liquid catalyst solution. The modified ionic liquid was obtained by reacting imidazolium with 3-(trimethoxysilyl)propyl chloride at 100 °C for 72 h. All catalyst systems showed good selectivity toward the branched aldehyde in the hydroformylation of vinylarenes, regardless of the electronic nature of the substrate (Figure 13). Due to the small pore size of 27 Å, a steric influence of the studied substrates was observed, with the more bulky ones causing a reduction in both rate and selectivity.

The branched to linear ratio was slightly influenced by the partial pressure of the syngas, with more branched aldehyde being formed under higher total pressures. Increasing the temperature resulted in a more significant decrease



**Figure 13.** Temperature and pressure dependence of vinylarene hydroformylation catalyzed by rhodium ionic liquid entrapped sol-gel catalysts. Reproduced based on data from ref 110. (Reaction conditions: syngas composition H<sub>2</sub>/CO<sub>2</sub> = 1:1, T = 50 °C, t = 12 h, 1.2 g of sol-gel catalyst, 1 mmol of vinylarene, 15 mL of alkane solvent).

of the branched aldehyde, accompanied by a higher overall reaction rate. The catalyst system has been recycled in four consecutive runs without loss of performance. However, after the fifth run, deterioration of the catalyst was observed, resulting in lower activity and selectivity.

### 5.1.2. Continuous Flow Reactions

The full technical potential of SILP catalysis has lately been extended to continuous flow processes with fixed-bed reaction designs.<sup>101</sup> Here, Rh-SILP catalyst systems modified with the charged phosphines cesium 3,4-dimethyl-2,5,6-tris-(*p*-sulfonatophenyl)-1-phosphanorbornadiene (NORBOS-Cs<sub>3</sub>) (**55**) and bis(*m*-phenylguanidinium)phenylphosphine hexafluorophosphate (**33**) (Scheme 10), which previously have been shown to be active and/or selective in biphasic liquid-liquid hydroformylation (*vide supra*), were used in a multiple layer of either [BMIM][PF<sub>6</sub>] or [BMIM][*n*-C<sub>8</sub>H<sub>17</sub>-OSO<sub>3</sub>] ionic liquid on amorphous silica for hydroformylation of propene and 1-octene.

First, a silica SILP Rh-**55**/[BMIM][PF<sub>6</sub>] catalyst was used for liquid, continuous-flow 1-octene hydroformylation in what essentially was a three-phase, syngas-organic liquid-ionic liquid fixed-bed reaction system. A steady catalyst performance corresponding to a TOF of 44 h<sup>-1</sup> and linearity around 72% *n*-nonanal was achieved after 3–4 h of reaction, albeit with low 1-octene conversion (<1%) restricted by the low solubility of the syngas in the 1-octene phase. No leaching of rhodium metal was detected by ICP analysis of outlet samples after this relatively short reaction time.

More comprehensive studies have been performed with the catalyst systems in propene gas-phase hydroformylation.<sup>102</sup> Here, the steady-state catalytic performance of analogous silica SILP catalysts based on the different ligands was initially found to be drastically influenced by the catalyst composition with respect to L/Rh ratio and ionic liquid loading, which both altered activity and selectivity, but rather independent of whether ionic liquids with [PF<sub>6</sub>]<sup>-</sup> or [*n*-C<sub>8</sub>H<sub>17</sub>-OSO<sub>3</sub>]<sup>-</sup> anions were contained in the catalyst phase. In particular, the catalyst systems based on sulfoxantphos ligand **7** (Scheme 4) proved interesting, as high linear product selectivity up to 96% was attained with these systems at high L/Rh ratios, indicating the presence of homogeneous catalyst

**Table 21. Hydroformylation of Propene<sup>a</sup> with SILP Silica Rh-phosphine/[BMIM][PF<sub>6</sub>] Catalysts<sup>101,102</sup>**

entry	ligand	L/Rh	ionic liquid loading		TOF (h <sup>-1</sup> )	<i>n</i> -butanal (%)
			wt %	$\alpha$		
191	<b>33</b>	2.9		0.00	55.5	47.4
192	<b>33</b>	2.9	108.4	0.78	20.6	47.4
193	<b>33</b>	2.9	138.9	1.00	16.8	50.0
194	<b>55</b>	11.3	6.9	0.05	88.4	66.7
195	<b>55</b>	11.3	20.8	0.15	79.4	56.5
196	<b>55</b>	21.4		0.00	45.8	73.8
197	<b>55</b>	21.3	6.9	0.05	28.2	72.2
198	<b>7</b>	2.5		0.00	37.4	63.0
199	<b>7</b>	2.4	23.6	0.17	1.5	64.0
200	<b>7</b>	2.5	68.1	0.49	5.1	66.4
201	<b>7</b>	10.2		0.00	40.8	94.4
202	<b>7</b>	10.0	25.0	0.18	34.9	95.8
203	<b>7</b>	10.0	72.2	0.52	25.4	95.8
204	<b>7</b>	20.0	27.8	0.20	16.7	96.0
205 <sup>b</sup>			105.6	0.76		

<sup>a</sup> Reaction conditions:  $p(\text{H}_2/\text{CO}/\text{C}_3\text{H}_6 = 1:1:1) = 5$  bar (entries 192–197) and 10 bar (entries 198–204),  $T = 100$  °C,  $t = 5$  h. SILP catalysts: 0.2 wt % Rh, dried silica gel (110 °C, 24 h, in vacuo), [BMIM][PF<sub>6</sub>] used for impregnation. <sup>b</sup> Support loaded with ionic liquid only.

complexes. With less ligand present, however, the selectivity was only comparable to the best selectivity obtained with the monodentate ligands using catalyst based on nonmodified silica support. It was realized that the catalysts deactivated by prolonged use, with a simultaneous decrease in catalytic activity and selectivity, independent of the type of ionic liquid, ionic liquid loading, and the L/Rh ratio comprised in the catalyst. This behavior was attributed to ligand degradation in the presence of the silica support material. Table 21 compiles steady-state results for the hydroformylation of propene with a series of different silica catalyst systems based on the ionic liquid [BMIM][PF<sub>6</sub>].

Riisager et al. have also studied the influence of the silica surface on catalyst stability and selectivity. Analogous silica Rh-sulfoxantphos/[BMIM][*n*-C<sub>8</sub>H<sub>17</sub>OSO<sub>3</sub>] catalysts (and catalysts without ionic liquid) were prepared using partially dehydroxylated support and subsequently used for continuous-flow propene hydroformylation reactions under similar reaction conditions as previously reported.<sup>103</sup> In contrast to the case of earlier catalysts based on nontreated support, the dehydroxylated catalysts containing ionic liquid (ionic liquid loading  $\alpha = 0.1$ ) were now found to maintain their initial maximum level of activity for more than 60 h on stream (i.e., TON > 2400) along with a high selectivity around 96% *n*-butanal. However, catalysts without ionic liquid still deactivated in prolonged reaction, probably as a consequence of slow surface diffusion of the ligand from the initial Rh-coordinated active state to a surface-bonded state, in which the metal atom is less coordinated to the ligand. Besides the

ionic liquid solvent, a relatively large excess of ligand was also found to be required for obtaining a stable catalyst system, even in reactions with pretreated support. This aspect was further recognized by solid-state <sup>29</sup>Si and <sup>31</sup>P MAS NMR to be directly related to an irreversible reaction of the ligand with the acidic silanol surface groups during catalysis. Moreover, FT-IR measurements on the supported catalysts under syngas at catalytic relevant conditions yielded CO bands assignable to the isomeric *ea/ee*-HRh(CO)<sub>2</sub>(**7**) complexes ( $\nu_{\text{CO}}^{\text{ea}} = 1994, 1948$  cm<sup>-1</sup>;  $\nu_{\text{CO}}^{\text{ee}} = 2035, 1964$  cm<sup>-1</sup>) analogous to those observed for related xanthene ligand-based rhodium complexes in organic and ionic liquid solvents (see Table 18), thus verifying the homogeneous complex formation in the SILP catalyst system. Additionally, the catalyst instability was established to be associated with degradation of the two isomeric complexes, which in turn was correlated to the accessible amount of ligand available for complex formation. Consequently, the prerequisites for obtaining an active, highly selective, and durable SILP hydroformylation catalyst were shown to involve both the presence of ionic liquid solvent and an excess of bisphosphine ligand to compensate for some detrimental surface reactions.

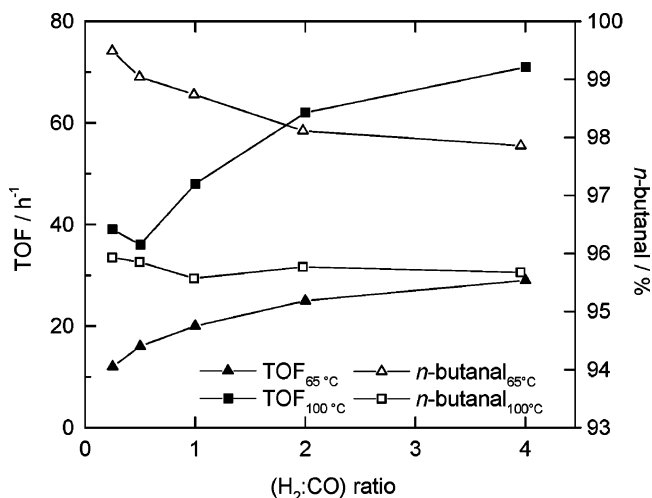
The long-term stability and the kinetics of the SILP hydroformylation catalysts have also been studied in continuous propene hydroformylation by Riisager and Haumann et al.<sup>104</sup> From variation of ionic liquid content in catalysts and parametrical changes of reaction conditions (e.g., reaction temperature and pressure, reactant concentrations, and residence time), the reaction rate was found to be independent of mass transport limitations from the gas into the liquid phase and allowed an activation energy of 63.3 (±2.1) kJ mol<sup>-1</sup> to be determined. This value is in good agreement with earlier results from homogeneous, biphasic hydroformylation in aqueous media, as shown in Table 22.

Variation in the syngas composition further established the pressure dependencies on the reaction rate to be first order in propene and fractional orders of 0.4 and -0.4 in H<sub>2</sub> and CO, respectively. These values are similar to those found in homogeneous hydroformylation that can be derived from the generally accepted Wilkinson mechanism for ligand modified rhodium catalysis.<sup>110–112</sup> Furthermore, the catalyst selectivity toward *n*-butanal was found only to be dependent on the syngas ratio at relatively low reaction temperatures (in contrast to the catalytic activity), where linear aldehyde could be formed practically exclusively (99.5%) with a 4-fold excess of CO gas, as shown in Figure 14. Such high selectivity has not been reported for Rh-**7** catalyst systems in either homogeneous or biphasic reaction systems, normally performed in batch autoclaves.<sup>113</sup> Under optimized reaction conditions, a steady-state catalyst performance corresponding

**Table 22. Activation Energies for Different Rh-Catalyzed Hydroformylation Systems<sup>104</sup>**

entry	substrate	catalyst	$E_a$ (kJ/mol)	solvent	support	ref
206	propene	SILP HRh(CO) <sub>2</sub> ( <b>7</b> ) <sup>a</sup>	63.2	[BMIM][ <i>n</i> -C <sub>8</sub> H <sub>17</sub> OSO <sub>3</sub> ]	SiO <sub>2</sub>	104
207	propene	HRh(CO)(TPPTS) <sub>3</sub>	77.0	water		105
208	1-octene	HRh(CO)(TPPTS) <sub>3</sub>	65.9	water		106
209	1-octene	HRh(CO)(TPPTS) <sub>3</sub>	71.0	water	SiO <sub>2</sub>	107
210	Linalool <sup>b</sup>	HRh(CO)(TPPTS) <sub>3</sub>	60.7	water	SiO <sub>2</sub>	108
211	1-dodecene	HRh(CO)(TPPTS) <sub>3</sub>	72.8/70.9 <sup>c</sup>	water <sup>d</sup>		109

<sup>a</sup> SILP catalysts: 0.2 wt % Rh, dehydroxylated silica gel (500 °C, 15 h, in vacuo), **7**/Rh = 10, [BMIM][*n*-C<sub>8</sub>H<sub>17</sub>OSO<sub>3</sub>] loading = 0.1). <sup>b</sup> Linalool: 3,7-dimethyl-1,6-octadien-3-ol. <sup>c</sup> Two different algorithms were used for data analysis. <sup>d</sup> CTAB (cetyltrimethylammonium bromide) surfactant used.



**Figure 14.** Effect on the syngas composition in the SILP Rh-7-catalyzed hydroformylation of propene. Reproduced from data in ref 113 (Reaction conditions:  $p(\text{H}_2/\text{CO} = 1:1) = 10$  bar, SILP catalysts: 0.2 wt % Rh, dehydroxylated silica gel (500 °C, 15 h, in vacuo), 7/Rh = 10, [BMIM][*n*-C<sub>8</sub>H<sub>17</sub>OSO<sub>3</sub>] loading = 0.1).

to an activity of TOF = 471 h<sup>-1</sup> and 94% linear selectivity could be obtained at 100 °C and 10 bar (H<sub>2</sub>/CO = 1:1) with a conversion degree about 20%.

The long-term stability of the SILP catalyst was further confirmed by unchanged selectivity during a week of continuous operation, despite the fact that a minor gradual decrease in activity (ca. 0.1% per hour) was observed as heavies (mainly aldol products), remaining dissolved in the ionic liquid catalyst phase, were formed, particularly at higher conversion. During extended operation, these heavies presumably reduced the effective catalyst concentration and increased the catalyst film thickness on the support, causing flooding of smaller pores and a lowering of the reaction surface. Since the selectivity remained unchanged, it was concluded that the catalyst complex was still intact, and short periodically exposure to vacuum could reactivate the catalyst and restore the initial catalyst performance.

The same authors have also studied the effect of carbon dioxide addition to the reactant gas.<sup>113</sup> CO<sub>2</sub> gas is known to have high solubility in most ionic liquids, lowering their viscosity and thus enhancing the diffusion of other gases.<sup>114,115</sup> The examination clearly demonstrated that the initial catalyst activity obtained without CO<sub>2</sub> cofeed could be increased by 2–35% by addition of 1.8–36.4 bar of CO<sub>2</sub> gas to the reactant stream containing a syngas pressure of 10 bar. In contrast, the initial selectivity was essentially not influenced (<1%) by the CO<sub>2</sub> addition and remained constant around 94.5% *n*-butanol with no detection of hydrogenated products being formed.

Recently, the SILP concept was further extended to continuous-flow, gas-phase 1-butene hydroformylation using the SILP Rh-sulfoxantphos/[BMIM][*n*-C<sub>8</sub>H<sub>17</sub>OSO<sub>3</sub>]/silica catalyst system.<sup>116</sup> The average reaction order with respect to partial pressure of 1-butene was found to be 1, whereas the H<sub>2</sub> partial pressure was found to have a positive effect on the reaction rate and the CO monoxide partial pressure a slightly negative one. All three observations are in accordance with the mechanism of homogeneous Rh-catalyzed hydroformylation, as is the case of SILP-catalyzed propene hydroformylation. Furthermore, variation of catalyst rhodium loading between 0.1 and 0.3 wt % revealed a linear dependency on the hydroformylation rate, indicating no

**Table 23. Comparison between SILP Rh-7-Catalyzed Hydroformylation<sup>a</sup> of Propene and 1-Butene<sup>116</sup>**

entry	substrate	$p_{\text{substrate}}$ (bar)	$T$ (°C)	TOF (h <sup>-1</sup> )	1-butene/propene <sup>b</sup>	<i>n</i> -aldehyde (%)
212	propene	2.1	100	103	2.5	95.6
213	1-butene	1.9	100	260		98.0
214	propene	2.1	120	308	2.1	94.8
215	1-butene	1.9	120	647		97.6

<sup>a</sup> Reaction conditions:  $p(\text{H}_2/\text{CO} = 1:1) = 10$  bar, residence time = 17 s. SILP catalysts: 0.2 wt % Rh, dehydroxylated silica gel (500 °C, 15 h, in vacuo), 7/Rh = 10, [BMIM][*n*-C<sub>8</sub>H<sub>17</sub>OSO<sub>3</sub>] loading = 0.1.  
<sup>b</sup> Ratio of TOF for 1-butene and propene.

limiting mass transport from the gas into the liquid phase. With these catalysts, the activation energy was calculated to be 63.8 kJ mol<sup>-1</sup>, in accordance with the value earlier obtained for the propene reaction, excluding additional pore diffusion of the larger substrate inside the SILP catalyst. However, when using catalysts with metal loading higher than 0.9 wt %, a lower effective activation energy of 55.2 kJ mol<sup>-1</sup> was found, indicating that the rate of gas–liquid transition in the catalyst pores became important, possibly due to an increased viscosity induced by the high ligand content.

A clear enhancement in both activity (about 2.5-fold up to 647 h<sup>-1</sup>) and selectivity from ca. 95% to 98% *n*-pentanal was observed for SILP-catalyzed hydroformylation of 1-butene compared to propene in the temperature range 100–120 °C. This activity difference was found to resemble the difference in the ratio of molar solubility (measured by a magnetic suspension balance) between propene and 1-butene in the ionic liquid phase in the SILP catalysts very closely, as shown in Table 23.

As earlier described (sections 2.1. and 2.2), the solubility of most gases is very low in ionic liquids. However, from the above results, it becomes obvious that in the case of SILP-catalyzed hydroformylation, no mass transport limitation from the gas into the ionic liquid phase can be observed, leaving the question where the reaction actually takes place in ionic liquid biphasic and SILP systems.

A first attempt to answer this question has been made by Steinrück et al. using X-ray photoelectron spectroscopy (XPS) studies on ionic liquid solutions of platinum complexes.<sup>117,118</sup> They reported the enrichment of platinum complexes at the ionic liquid [EMIM][C<sub>2</sub>H<sub>5</sub>OSO<sub>3</sub>]-vacuum interface with the bulk of the ionic liquid phase being depleted from platinum. If this observation holds true under reaction conditions, the hydroformylation (and hydrogenation) would become a surface reaction and therefore be less influenced by the gas solubility, which would explain adequately why reactions in ionic liquids proceed readily despite the poor gas solubility of especially H<sub>2</sub> gas. Recently, molecular dynamics studies on biphasic ionic liquid–organic systems<sup>95</sup> have further indicated this depletion effect. Thus, clearly, much more work has to be done in this respect in order to find optimized reaction conditions—not only for hydroformylation.

## 5.2. Ionic Liquid–Supercritical CO<sub>2</sub> Systems

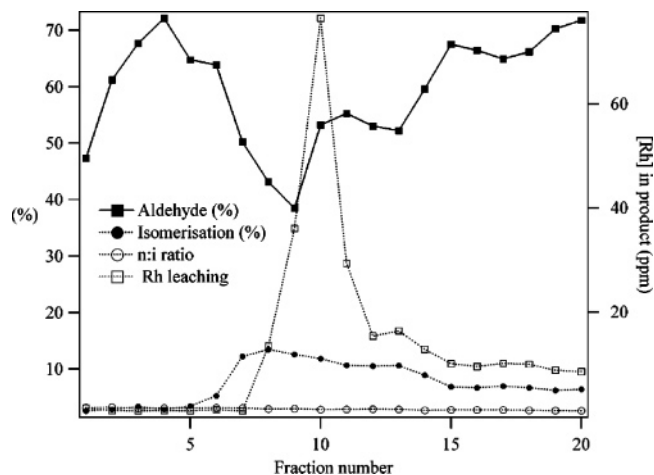
### 5.2.1. Biphasic-Catalyzed Reactions

As described in the previous section, supported ionic liquid-phase Rh catalyst systems are only ideally suited for continuous, gas-phase applications of vaporizable substrates due to possible catalyst leaching in liquid systems. Another

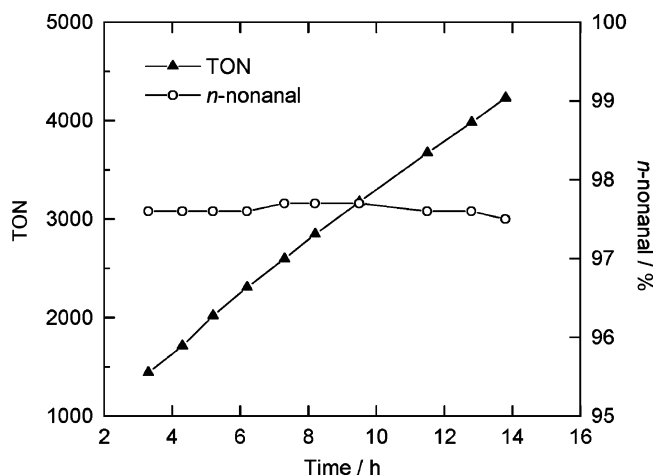
recent development allowing continuous-flow, hydroformylation of liquid, long-chained alkenes has, however, been developed by Cole-Hamilton and co-workers.<sup>119</sup> They have applied a concept involving use of biphasic ionic liquid/scCO<sub>2</sub> (scCO<sub>2</sub>: supercritical CO<sub>2</sub>) systems where alkene, syngas, and scCO<sub>2</sub> (either separately or mixed) are passed into a tank reactor containing an ionic liquid with a dissolved ionic Rh catalyst. Here, reaction is efficiently enhanced, since scCO<sub>2</sub> is typically very soluble in ionic liquid phases, while the ionic liquid is essentially insoluble in scCO<sub>2</sub>.<sup>114,115</sup> At the end of the reaction, the products flow out of the reactor dissolved in scCO<sub>2</sub>, leaving behind the ionic liquid catalyst phase in the reactor due to its insolubility in scCO<sub>2</sub>. Finally, the product stream is decompressed to release the products, and eventually the CO<sub>2</sub> containing any excess syngas can be recompressed for an emission free and continuous process that requires no further product or catalyst separation.

The first successful continuous hydroformylation performed using the described biphasic ionic liquid/scCO<sub>2</sub> systems was reported by Cole-Hamilton et al. with 1-octene using a Rh<sub>2</sub>(OAc)<sub>4</sub>[PhP(C<sub>6</sub>H<sub>4</sub>SO<sub>3</sub>)<sub>2</sub>][PMIM]<sub>2</sub> **56** catalyst system (**56**/Rh = 16) dissolved in [BMIM][PF<sub>6</sub>] at 100 °C and 40 bar syngas (H<sub>2</sub>/CO = 1:1) at 200 bar total pressure.<sup>120</sup> During 33 h of continuous hydroformylation, the catalyst activity was found to remain constant but modest, with a TOF of 8 h<sup>-1</sup>, with no indication of catalyst decomposition (in contrast to initial studies on 1-hexene and 1-nonene with aryl phosphite ligands, where HF, formed from hydrolysis of the ionic liquid by water traces, led to ligand degradation<sup>119</sup>). Moreover, Rh leaching into the scCO<sub>2</sub>/product stream was found to be less than 1 ppm, and the selectivity toward *n*-nonanal remained constant around 76% throughout the reaction with no occurrence of ligand oxidation. Ligand oxidation had, in preliminary reactions performed in repetitive batch mode with successive catalyst recycling, resulted in significant Rh leaching due to formation of unmodified HRh(CO)<sub>4</sub> **57** catalyst which displays some solubility in scCO<sub>2</sub>. This resulted in a continuous decrease of catalyst selectivity (from 79% to 71%) and increased isomerization activity (up to 20%).

In further studies using the Rh-phosphine catalyst **56**, the productivity of the continuous hydroformylation reaction was optimized with respect to reaction parameters using terminal C<sub>8</sub>–C<sub>12</sub> alkenes and styrene as substrates.<sup>121</sup> By systematically increasing the alkyl chain length on the ionic liquid cation and the anion in the ionic liquid, [OMIM][Tf<sub>2</sub>N] was found to be the most effective solvent, providing a rate increase as a result of increased solubility of long-chained alkenes. Furthermore, increasing the flow rate through the system, and hence the partial pressure of CO and H<sub>2</sub>, increased the reaction rate as the solvating power of the mobile phase decreased, thus allowing more substrate to partition in the catalyst phase. However, an upper limit of the partial pressures of the reactants, corresponding to what effectively can be used for reaction, was found, which in turn was determined by the ability of the scCO<sub>2</sub> phase to extract reaction products. Thus, at very high syngas partial pressures, the reaction system was limited when the rate of product dissolution by the mobile phase was insufficient to remove it at a rate equivalent to that at which it is formed. Nevertheless, optimized conditions allowed a TOF of 517 h<sup>-1</sup> to be achieved, which is significantly higher than that obtained for present commercial hydroformylation systems of higher alkenes. Furthermore, the catalyst proved stable



**Figure 15.** Effect of changing syngas composition during the continuous Rh-catalyzed hydroformylation of 1-octene using a [OMIM][Tf<sub>2</sub>N]/scCO<sub>2</sub> reaction system. Reproduced with permission from ref 121. Copyright 2003 American Chemical Society. (Reaction conditions:  $p(\text{H}_2/\text{CO} = 1:1) = 40$  bar,  $p_{\text{total}} = 200$  bar,  $F_{1\text{-octene}} = 0.76$  mmol min<sup>-1</sup>,  $F_{\text{CO}_2} = 1.00$  nL min<sup>-1</sup>,  $F_{\text{CO}} = 1.86$  mmol min<sup>-1</sup> (fraction 1–5),  $F_{\text{CO}} = 0.8$  mmol min<sup>-1</sup> (fraction 6–9),  $F_{\text{CO}} = 1.12$  mmol min<sup>-1</sup> (fraction 10–13),  $F_{\text{CO}} = 1.86$  mmol min<sup>-1</sup> (fraction 14–17), and  $F_{\text{CO}} = 2.66$  mmol min<sup>-1</sup> (fraction 18–20). Catalyst system: 49.2 mg Rh(acac)(CO)<sub>2</sub>, 1.31 g of [PhP(C<sub>6</sub>H<sub>4</sub>SO<sub>3</sub>)<sub>2</sub>][PMIM]<sub>2</sub> (**56**) (**56**/Rh = 15), 12 mL of [OMIM][Tf<sub>2</sub>N].)

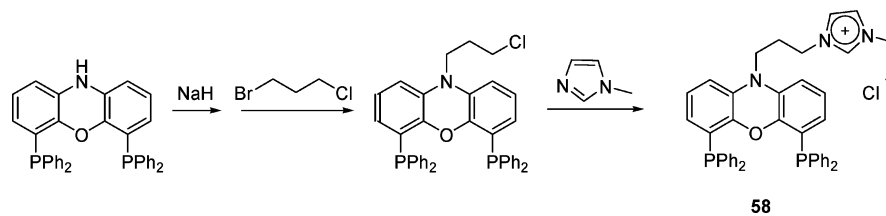


**Figure 16.** Continuous Rh-catalyzed hydroformylation of 1-octene using a [OMIM][Tf<sub>2</sub>N]/scCO<sub>2</sub> reaction system with ligand **58**. Reproduced based on data from ref 121. (Reaction conditions:  $p(\text{H}_2/\text{CO} = 1:1) = 40$  bar,  $p_{\text{total}} = 200$  bar,  $T = 100$  °C. Catalyst system: Rh(acac)(CO)<sub>2</sub>, ligand **58** and [OMIM][Tf<sub>2</sub>N].)

for 72 h of continuous operation, yielding constant rate, and selectivity between 75 and 78%, and an average low Rh metal leaching of less than 0.1 ppm. The metal leaching was, however, also prone to variation depending on the applied reactant partial pressures, because lower pressures resulted in increased solubility of both the substrate and the catalyst in scCO<sub>2</sub>. Moreover, the purity of the compressed CO<sub>2</sub> gas used to make the scCO<sub>2</sub> was also found to affect the Rh leaching—as well as the amount of isomerization products—presumably due to traces of oxidized phosphine ligand formed by impurities in the CO<sub>2</sub> gas, resulting in formation of **57**, as also observed in earlier studies.<sup>120</sup> In Figure 15 the effect of changing the partial pressure through variation of the flow rates of syngas is shown for the reaction of 1-octene.

The linear selectivity in the biphasic 1-octene hydroformylation ionic liquid/scCO<sub>2</sub> reaction was further improved, as shown in Figure 16, when the original catalyst system

**Scheme 19. Preparation Route to 4,6-Bis(diphenylphosphino)phenoxazine Ligand (Nixantphos) Modified with a 3-Propylimidazolium Ionic Tag<sup>a</sup>**



<sup>a</sup> The detailed synthesis procedure can be found in ref 121.

**Table 24. Comparison of Commercial and Ionic Liquid/scCO<sub>2</sub> 1-Octene Hydroformylation System<sup>122</sup>**

entry	process characteristics	BASF process	Shell process	ionic liquid /scCO <sub>2</sub> <sup>a</sup>
216	substrate	1-octene	1-octene	1-octene
217	ligand	none	<i>P</i> (butyl) <sub>3</sub>	<b>58</b>
218	[Rh] (mmol L <sup>-1</sup> )	80	80	15
219	<i>p</i> (bar)	300	80	200
220	<i>T</i> (°C)	150	200	100
221	STY <sup>b</sup> (h <sup>-1</sup> )	0.5	0.3	0.74 (1.4)
222	rate (mol L <sup>-1</sup> h <sup>-1</sup> )	2.8	1.8	4.1 (7.8)
223	TOF (h <sup>-1</sup> )	35	20	272 (517)
224	linear aldehyde (%)	50	80	92 (75)

<sup>a</sup> Optimized values obtained with catalyst system **56** (Rh<sub>2</sub>(OAc)<sub>4</sub>-[PhP(C<sub>6</sub>H<sub>4</sub>SO<sub>3</sub>)<sub>2</sub>]<sub>2</sub>[PMIM]<sub>2</sub> in [BMIM][PF<sub>6</sub>]) are given in parentheses.  
<sup>b</sup> Space time yield as liters of product per liter of catalyst solution.

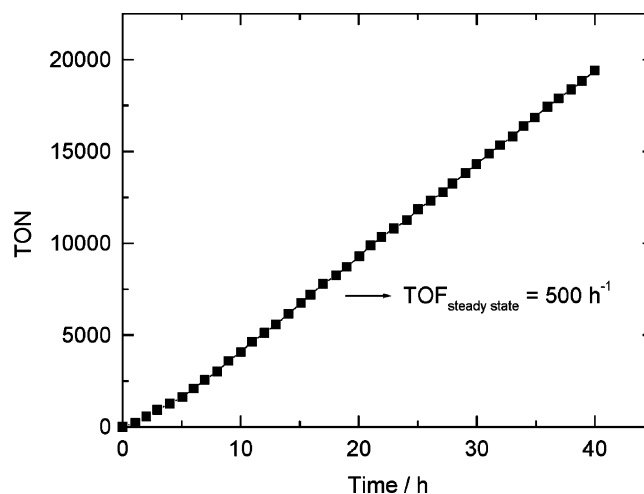
involving the monophosphine ligand [PhP(C<sub>6</sub>H<sub>4</sub>SO<sub>3</sub>)<sub>2</sub>]-[PMIM]<sub>2</sub> (**56**) was changed for the bisphosphine ligand **58** containing a xanthene skeleton (nixantphos) with an ionic liquid tag, prepared by the route shown in Scheme 19.<sup>121</sup>

Here, a constant selectivity around 97.6% *n*-nonanal and a steady-state TOF of 272 h<sup>-1</sup> were maintained for more than 15 h of reaction. However, the selectivity dropped dramatically after longer reaction times due to ligand oxidation (confirmed by NMR), and rhodium leaching of about 0.2 ppm was slightly higher than that observed using the initial catalyst system containing monophosphine ligand. Nevertheless, the optimized ionic liquid/scCO<sub>2</sub> biphasic process using the modified nixantphos ligand **58** compared favorably with present commercial 1-octene hydroformylation processes using cobalt-based catalysts (with or without modifying phosphine ligand), as shown in Table 24, where some key features of the reaction systems are compared.

### 5.2.2. SILP-Catalyzed Reactions

Recently, Cole-Hamilton and co-workers further combined the SILP catalysis concept (see section 5.1 for details) with the use of scCO<sub>2</sub> as transport vector for carrying out 1-octene hydroformylation in a continuous-flow, fixed-bed reaction system.<sup>123,124</sup> Initial results obtained with the established **56**/[OMIM][Tf<sub>2</sub>N] catalyst system supported on silica at 100 °C and 100 bar total pressure yielded selectivity around 76% *n*-nonanal, as also previously found in the analogous biphasic ionic liquid/scCO<sub>2</sub> reaction system.<sup>120</sup> More interestingly, very high reaction rates corresponding to TOF of 500–800 h<sup>-1</sup> could be maintained for at least 40 h of continuous flow operation (TONs > 20000) independent of ionic liquid loading on the SILP catalyst (but dependent on the substrate flow with higher rates at higher flows), as exemplified in Figure 17.

The results confirmed that the reaction was not limited by mass transport into the ionic liquid phase, and they further indicated that inhibiting low-volatile aldol products, which



**Figure 17.** Cumulative turnover number for continuous, fixed-bed Rh-catalyzed hydroformylation of 1-octene using a silica SILP **56**-[OMIM][Tf<sub>2</sub>N]/scCO<sub>2</sub> reaction system. Reproduced based on data from ref 123. (Reaction conditions: *p*(H<sub>2</sub>/CO = 1:1) = 40 bar, *p*<sub>total</sub> = 100 bar, *T* = 100 °C, *F*<sub>1-octene</sub> = 0.42 cm<sup>3</sup> min<sup>-1</sup>, *F*<sub>total</sub> = 854 cm<sup>3</sup> min<sup>-1</sup>, H<sub>2</sub>/CO:1-octene = 10.)

eventually may have formed during the reaction, were efficiently removed from the supported ionic liquid catalyst layer by the scCO<sub>2</sub> product stream. No genuine rhodium metal leaching measurements have so far been reported for the solid catalyst system to establish whether the metal inventory remains sufficiently immobilized in the ionic liquid phase during operation. However, analyses by NMR and ICPMS have revealed traces of both ionic liquid and Rh metal (up to 4 ppm) in some of the collected samples.

## 6. Concluding Comments

As shown in this review, significant progress in recent years has now allowed biphasic ionic liquid hydroformylation catalysts to be engineered—by careful choice of ionic liquid and through rational ligand design—to provide very effective catalyst immobilization and acquire optimized catalytic performance. Detailed spectroscopic characterization has further established the complex chemistry in ionic liquid hydroformylation catalysts to be identical to the complex formation in traditional solvent systems. Moreover, reaction systems requiring only CO<sub>2</sub>, H<sub>2</sub>, and alkene, without need for toxic CO or any volatile organic solvents, have recently been introduced as an attractive protocol for carrying out hydroformylation in a benign manner.

However, ionic liquids generally exhibit rather low syngas solubility, which makes biphasic hydroformylation systems prone to mass transfer limitations. In such cases, most parts of the reaction are restricted to the diffusion layer of the ionic liquid catalyst phase rather than the bulk solvent, resulting in inefficient use of both expensive ionic liquid and

precious metal catalyst. Supported ionic liquid-phase (SILP) catalyst systems and combined ionic liquid–scCO<sub>2</sub> catalyst systems can, however, circumvent these transport problems by enabling an improved contact between the ionic liquid catalyst phase and the syngas, thus making diffusion issues much less important. Importantly, process intensification and improved catalyst materials utilization have also proven possible with these catalyst systems when implemented into continuous-flow, fixed-bed reaction design.<sup>125</sup>

## 7. Acknowledgements

Financial support by the Deutsche Forschungsgemeinschaft (M.H.), the Danish Research Council for Technology and Production, and the Lundbeck Foundation (A.R.) is gratefully acknowledged. The authors further thank Prof. P. Wasserscheid, University of Erlangen-Nürnberg, and Prof. R. Fehrmann, Technical University of Denmark, for their advice and contributions in connection with writing of the manuscript.

## 8. References

- Holbrey, J. D.; Seddon, K. R. *Clean Prod. Proc.* **1999**, *1*, 223.
- Welton, T. *Chem. Rev.* **1999**, *99*, 2071.
- Dupont, J.; Consorti, C. S.; Spencer, J. *J. Braz. Chem. Soc.* **2000**, *11*, 337.
- Wasserscheid, P.; Keim, W. *Angew. Chem., Int. Ed.* **2000**, *39*, 3772.
- Tzschucke, C. C.; Markert, C.; Bannwarth, W.; Roller, S.; Hebel, A.; Haag, R. *Angew. Chem., Int. Ed.* **2000**, *41*, 3964.
- Wasserscheid, P.; Welton, T., Eds. *Ionic Liquids in Synthesis*, 2nd ed.; Wiley-VCH: Weinheim, 2007.
- Cornils, B.; Wiebus, E. *CHEMTECH* **1995**, *25*, 33.
- Cornils, B.; Herrmann, W. A.; Eckl, R. W. *J. Mol. Catal., A: Chem.* **1997**, *116*, 27.
- Kohlpaintner, C. W.; Fischer, R. W.; Cornils, B. *Appl. Catal., A* **2001**, *221*, 219.
- Scammells, P. J.; Scott, J. L.; Singer, R. D. *Aust. J. Chem.* **2005**, *58*, 155.
- vanWazer, J. R. *Phosphorous and Its Compounds*; Wiley: New York, 1958; Vol. 1.
- Swatloski, R. P.; Holbrey, J. D.; Rogers, R. D. *Green Chem.* **2003**, *5*, 361.
- Fonseca, G. S.; Umpierre, A. P.; Fichtner, P. F. P.; Teixeira, S. R.; Dupont, J. *Chem.—Eur. J.* **2003**, *9*, 3263.
- Wiebus, E.; Cornils, B. *Biphasic Systems: Water-Organic in Catalyst Separation, Recovery and Recycling*; Catalysis by Metal Complexes, Vol. 30; Cole-Hamilton, D., Tooze, R., Eds.; Springer: Dordrecht, 2006.
- Wasserscheid, P.; Haumann, M. Catalyst Recycling Using Ionic Liquids. In *Catalyst Separation, Recovery and Recycling*; Catalysis by Metal Complexes, Vol. 30; Cole-Hamilton, D., Tooze, R., Eds.; Springer: Dordrecht, 2006.
- Wasserscheid, P. *J. Ind. Eng. Chem.* **2007**, *13*, 325.
- Parshall, G. W. *J. Am. Chem. Soc.* **1972**, *94*, 8716.
- Knifton, J. F. *J. Mol. Catal.* **1987**, *43*, 65.
- Karodia, N.; Guise, S.; Newlands, C.; Andersen, J. *Chem. Commun.* **1998**, 2341.
- Chauvin, Y.; Musmann, L.; Olivier, H. *Angew. Chem., Int. Ed.* **1995**, *34*, 2698.
- <http://www.cas.org/SCIFINDER/>, search keywords “ionic liquids”, December 2007.
- Sheldon, R. *Chem. Commun.* **2001**, 2399.
- Gordon, C. M. *Appl. Catal., A* **2001**, *222*, 101.
- Zhao, H.; Malhotra, S. V. *Aldrichim. Acta* **2002**, *35*, 75.
- Welton, T. *Coord. Chem. Rev.* **2004**, *248*, 2459.
- Dyson, P. J. *Transition Met. Chem.* **2002**, *27*, 353.
- Zhao, D.; Wu, M.; Kou, Y.; Min, E. *Catal. Today* **2002**, *74*, 157.
- Dupont, J.; de Souza, R. F.; Suarez, P. A. Z. *Chem. Rev.* **2002**, *102*, 3667.
- Olivier-Bourbigou, H.; Magna, L. *J. Mol. Catal., A* **2002**, *419*, 182–183.
- Parvulescu, I. V.; Hardacre, C. *Chem. Rev.* **2007**, *107*, 2615.
- Cornils, B.; Herrmann, W. A.; Horvath, I. T.; Leitner, W.; Mecking, S.; Olivier-Bourbigou, H.; Vogt, D., Eds. *Multiphase Homogeneous Catalysis*; Wiley-VCH: Weinheim, 2005; Vol. 2.
- Dyson, P. J.; Geldbach, T. J., Eds. *Metal Catalyzed Reactions in Ionic Liquids*; Catalysis by Metal Complexes, Vol. 29; Springer: Dordrecht, 2005.
- Adams, D. J.; Dyson, P. J.; Tavener, S. J. *Chemistry in Alternative Reaction Media*; John Wiley & Sons: West Sussex, 2004.
- Baerns, M.; Claus, P. *Chemical Reaction Engineering Aspects of Homogeneously Catalyzed Reactions in Applied Homogeneous Catalysis with Organometallic Compounds*; Cornils, B., Herrmann, W. A., Eds.; Wiley-VCH: Weinheim, 2002.
- Berger, A.; de Souza, R. F.; Delgado, M. R.; Dupont, J. *Tetrahedron: Asymmetry* **2001**, *12*, 1825.
- Anthony, J. L.; Maginn, E. J.; Brennecke, J. F. *J. Phys. Chem. B* **2002**, *106*, 7315.
- Dyson, P. J.; Laurenczy, G.; Ohlin, C. A.; Vallance, J.; Welton, T. *Chem. Commun.* **2003**, 2418.
- Kumelan, J.; Pérez-Salado Kamps, A.; Tuma, D.; Maurer, G. *J. Chem. Eng. Data* **2006**, *51*, 1364.
- Jacquemin, J.; Costa Gomes, M. F.; Husson, P.; Majer, V. *J. Chem. Thermodyn.* **2006**, *38*, 490.
- Ohlin, C. A.; Dyson, P. J.; Laurenczy, G. *Chem. Commun.* **2004**, 1070.
- Kumelan, J.; Pérez-Salado Kamps, A.; Tuma, D.; Maurer, G. *Fluid Phase Equilib.* **2005**, *228–229*, 207.
- Camper, D.; Becker, C.; Koval, C.; Noble, R. *Ind. Eng. Chem. Res.* **2005**, *44*, 1928.
- Camper, D.; Becker, C.; Koval, C.; Noble, R. *Ind. Eng. Chem. Res.* **2006**, *45*, 445.
- Lee, B.; Outcalt, S. L. *J. Chem. Eng. Data* **2006**, *51*, 892.
- Frohning, C. D.; Kohlpaintner, C. W. Hydroformylation. In *Applied Homogeneous Catalysis with Organometallic Compounds*; Cornils, B., Herrmann, W. A., Eds.; Wiley-VCH: Weinheim, 2002.
- Wachsen, O.; Himmler, K.; Cornils, B. *Catal. Today* **1998**, *42*, 373.
- Sumartschenkowa, I. A.; Verevkin, S. P.; Vasiltsova, T. V.; Bich, E.; Heintz, A.; Shevelyova, M. P.; Kabo, G. J. *J. Chem. Eng. Data* **2006**, *51*, 2138.
- Heintz, A.; Kulikov, D. V.; Verevkin, S. P. *J. Chem. Eng. Data* **2002**, *47*, 894.
- Krummen, M.; Wasserscheid, P.; Gmehling, J. *J. Chem. Eng. Data* **2002**, *47*, 1411.
- Heintz, A.; Casás, L. M.; Nesterov, I. A.; Emel'yanenko, V. N.; Verevkin, S. P. *J. Chem. Eng. Data* **2005**, *50*, 1510.
- Heintz, A.; Verevkin, S. P.; Ondo, D. *J. Chem. Eng. Data* **2006**, *51*, 434.
- Kato, R.; Gmehling, J. *J. Chem. Thermodyn.* **2005**, *37*, 603.
- Foco, G. M.; Bottini, S. B.; Quezada, N.; de la Fuente, J. C.; Peters, C. J. *J. Chem. Eng. Data* **2006**, *51*, 1088.
- Zhou, Q.; Wang, L.-S.; Wu, J.-S.; Li, M.-Y. *J. Chem. Eng. Data* **2007**, *52*, 131.
- Keim, W.; Vogt, D.; Waffenschmidt, H.; Wasserscheid, P. *J. Catal.* **1999**, *186*, 481.
- Wasserscheid, P.; Waffenschmidt, H. *J. Mol. Catal., A* **2000**, *164*, 61.
- Favre, F.; Olivier-Bourbigou, H.; Commereuc, D.; Saussine, L. *Chem. Commun.* **2001**, 1360.
- Dupont, J.; Silva, S. M.; de Souza, R. F. *Catal. Lett.* **2001**, *77*, 131.
- Wasserscheid, P.; van Hal, R.; Bösmann, A. *Green Chem.* **2002**, *4*, 400.
- Dupont, J.; Spencer, J. *Angew. Chem., Int. Ed.* **2004**, *43*, 5296.
- Stenzel, O.; Raubenheimer, H. G.; Esterhuysen, C. *J. Chem. Soc., Dalton Trans.* **2002**, 1132.
- Omotowa, B. A.; Shreeve, J. M. *Organometallics* **2004**, *23*, 783.
- Kong, F.; Jiang, J.; Jin, Z. *Catal. Lett.* **2004**, *96*, 63.
- Williams, D. B. G.; Ajam, M.; Ranwell, A. *Organometallics* **2007**, *26*, 4692.
- Lin, Q.; Jiang, W.; Fu, H.; Chen, H.; Li, X. *Appl. Catal., A* **2007**, *328*, 83.
- Brasse, C. C.; Englert, U.; Salzer, A.; Waffenschmidt, H.; Wasserscheid, P. *Organometallics* **2000**, *19*, 3818.
- Herberich, G. E.; Greiss, G. *J. Organomet. Chem.* **1971**, *27*, 113.
- Coville, N. J.; du Plooy, K. E.; Pickl, W. *Coord. Chem. Rev.* **1992**, *116*, 1.
- Brauer, D. J.; Kottsieper, K. W.; Liek, C.; Stelzer, O.; Waffenschmidt, H.; Wasserscheid, P. *J. Organomet. Chem.* **2001**, *630*, 177.
- Wasserscheid, P.; Waffenschmidt, H.; Machnitzki, P.; Kottsieper, K. W.; Stelzer, O. *Chem. Commun.* **2001**, 451.
- Bronger, R. P. J.; Silva, S. M.; Kamer, P. C. J.; van Leeuwen, P. W. N. M. *Chem. Commun.* **2002**, 3044.
- van Leeuwen, P. W. N. M.; Claver, C., Eds. *Rhodium Catalyzed Hydroformylation*; Catalysis by Metal Complexes, Vol. 22; Springer: Dordrecht, 2000.
- Bronger, R. P. J.; Silva, S. M.; Kamer, P. C. J.; van Leeuwen, P. W. N. M. *Dalton Trans.* **2004**, 1590.



- (74) Peng, Q.; Deng, C.; Yang, Y.; Dai, M.; Yuan, Y. *React. Kinet. Catal. Lett.* **2007**, *90*, 53.
- (75) Deng, C.; Ou, G.; She, J.; Yuan, Y. *J. Mol. Catal., A* **2007**, *270*, 76.
- (76) Köckritz, A.; Bischoff, S.; Kant, M.; Siefken, R. *J. Mol. Catal., A* **2001**, *174*, 119.
- (77) Tominaga, K.; Sasaki, Y. *Catal. Commun.* **2000**, *1*, 1.
- (78) Tominaga, K.; Sasaki, Y. *J. Mol. Catal., A* **2004**, *220*, 159.
- (79) Tominaga, K.; Sasaki, Y.; Hagihara, K.; Watanabe, T.; Saito, M. *Chem. Lett.* **1994**, 1391.
- (80) Tominaga, K.; Sasaki, Y. *Recent Res. Dev. Pure Appl. Chem.* **1998**, *2*, 217.
- (81) Tominaga, K.; Sasaki, Y. *Chem. Lett.* **2004**, *33*, 14.
- (82) Tominaga, K.; Sasaki, Y. *Stud. Surf. Sci. Catal.* **2004**, *153*, 227.
- (83) Tominaga, K. *Catal. Today* **2006**, *115*, 70.
- (84) Ford, P. C.; Massick, S. *Coord. Chem. Rev.* **2002**, *226*, 39.
- (85) Dwyer, C.; Assumption, H.; Cotzee, J.; Crause, C.; Damoense, L.; Kirk, M. *Coord. Chem. Rev.* **2004**, *248*, 653.
- (86) Damoense, L.; Datt, M.; Green, M.; Steenkamp, C. *Coord. Chem. Rev.* **2004**, *248*, 2393.
- (87) Kamer, P. C.; van Rooy, A.; Schoemaker, G. C.; van Leeuwen, P. W. N. M. *Coord. Chem. Rev.* **2004**, *248*, 2409.
- (88) Silva, S. M.; Bronger, R. P. J.; Freixa, Z.; Dupont, J.; van Leeuwen, P. W. N. M. *New J. Chem.* **2003**, *27*, 1294.
- (89) van der Veen, L. A.; Boele, M. D. K.; Bregman, F. R.; Kamer, P. C. J.; van Leeuwen, P. W. N. M.; Goubitz, K.; Fraanje, J.; Schenk, H.; Bo, C. *J. Am. Chem. Soc.* **1998**, *120*, 11616.
- (90) van der Veen, L. A.; Keeven, P. H.; Schoemaker, G. C.; Reek, J. N. H.; Kamer, P. C. J.; van Leeuwen, P. W. N. M.; Lutz, M.; Spek, A. L. *Organometallics* **2000**, *19*, 872.
- (91) Goedheijt, M. S.; Kamer, P. C. J.; van Leeuwen, P. W. N. M. *J. Mol. Catal., A* **1998**, *134*, 243.
- (92) Mehnert, C. P.; Cook, R. A.; Dispenziere, N. C.; Mozeleski, E. J. *Polyhedron* **2004**, *23*, 2679.
- (93) Horvath, I. T.; Kastup, R. V.; Oswald, A. A.; Mozeleski, E. J. *Catal. Lett.* **1989**, *2*, 85.
- (94) Cornils, B.; Herrmann, W. A., Eds. *Aqueous-Phase Organometallic Catalysis*; Wiley-VCH: Weinheim, 2004.
- (95) Sieffert, N.; Wipff, G. *J. Phys. Chem. B* **2007**, *111*, 4951.
- (96) Illner, P.; Zahl, A.; Puchta, R.; van Eikemma Hommes, N.; Wasserscheid, P.; van Eldik, R. *J. Organomet. Chem.* **2005**, *690*, 3567.
- (97) Mehnert, C. P.; Cook, R. A.; Dispenziere, N. C.; Afeworki, M. *J. Am. Chem. Soc.* **2002**, *124*, 12932.
- (98) Yang, Y.; Lin, H.; Deng, C.; She, J.; Yuan, Y. *Chem. Lett.* **2005**, *34*, 220.
- (99) Yang, Y.; Deng, C.; Yuan, Y. *J. Catal.* **2005**, *232*, 108.
- (100) Hamza, K.; Blum, J. *Eur. J. Org. Chem.* **2007**, 4706.
- (101) Riisager, A.; Eriksen, K. M.; Wasserscheid, P.; Fehrmann, R. *Catal. Lett.* **2003**, *90*, 149.
- (102) Riisager, A.; Wasserscheid, P.; van Hal, R.; Fehrmann, R. *J. Catal.* **2003**, *219*, 452.
- (103) Riisager, A.; Fehrmann, R.; Flicker, S.; van Hal, R.; Haumann, M.; Wasserscheid, P. *Angew. Chem., Int. Ed.* **2005**, *44*, 185.
- (104) Riisager, A.; Fehrmann, R.; Haumann, M.; Gorle, B. S. K.; Wasserscheid, P. *Ind. Eng. Chem. Res.* **2005**, *44*, 9853.
- (105) Yang, C.; Mao, Z. S.; Wang, Y.; Chen, J. *Catal. Today* **2002**, *74*, 111.
- (106) Desphande, R. M.; Purwanto; Delmas, H.; Chaudhari, R. V. *Ind. Eng. Chem. Res.* **1996**, *35*, 3927.
- (107) Jáuregui-Haza, U. J.; Pardillo-Fontdevila, E.; Kalck, P. *Catal. Today* **2003**, *409*, 79–80.
- (108) Benaissa, M.; Jáuregui-Haza, U. J.; Nikovc, I.; Wilhelm, A. M.; Delmas, H. *Catal. Today* **2003**, *419*, 79–80.
- (109) Zhang, Y.; Mao, Z. S.; Chen, J. *Catal. Today* **2002**, *74*, 23.
- (110) Young, J. F.; Osborn, J. A.; Jardine, F. A.; Wilkinson, G. *J. Chem. Soc., Chem. Commun.* **1965**, 131.
- (111) Evans, D.; Osborn, J. A.; Wilkinson, G. *J. Chem. Soc.* **1968**, 3133.
- (112) Evans, D.; Yagupsky, G.; Wilkinson, G. *J. Chem. Soc.* **1968**, 2660.
- (113) Riisager, A.; Fehrmann, R.; Haumann, M.; Wasserscheid, P. *Eur. J. Inorg. Chem.* **2006**, 695.
- (114) Cadena, C.; Anthony, J. L.; Shah, J. K.; Morrow, T. I.; Brennecke, J. F.; Maginn, E. J. *J. Am. Chem. Soc.* **2004**, *126*, 5300.
- (115) Solinas, M.; Pfaltz, A.; Cozzi, P.; Leitner, W. *J. Am. Chem. Soc.* **2004**, *126*, 16142.
- (116) Haumann, M.; Dentler, K.; Joni, J.; Riisager, A.; Wasserscheid, P. *Adv. Synth. Catal.* **2007**, *349*, 425.
- (117) Maier, F.; Gottfried, J. M.; Rossa, J.; Gerhard, D.; Schulz, P. S.; Schwieger, W.; Wasserscheid, P.; Steinrueck, H.-P. *Angew. Chem., Int. Ed.* **2006**, *45*, 7778.
- (118) Gottfried, J. M.; Maier, F.; Rossa, J.; Gerhard, D.; Schulz, P. S.; Wasserscheid, P.; Steinrueck, H.-P. *Z. Phys. Chem.* **2006**, *220*, 1439.
- (119) Sellin, M. F.; Cole-Hamilton, D. J. *J. Chem. Soc., Dalton Trans.* **2000**, 1681.
- (120) Sellin, M. F.; Webb, P. B.; Cole-Hamilton, D. J. *Chem. Commun.* **2001**, 781.
- (121) Webb, P. B.; Sellin, M. F.; Kunene, T. E.; Williamson, S.; Slawin, A. M. Z.; Cole-Hamilton, D. J. *J. Am. Chem. Soc.* **2003**, *125*, 15577.
- (122) Webb, P. B.; Kunene, T. E.; Cole-Hamilton, D. J. *Green Chem.* **2005**, *7*, 373.
- (123) Cole-Hamilton, D. J.; Desset, S. L.; Hintermair, U.; Santini, C. C.; Muldoon, M. J. *Proceedings of the DGMK/SCI-Conference Synthesis Gas Chemistry*, 2006; p 41.
- (124) Hintermair, U.; Zhao, G.; Santini, C. C.; Muldoon, M. J.; Cole-Hamilton, D. J. *Chem. Commun.* **2007**, 1462.
- (125) www.silp-technology.com.

CR078374Z